Geologic Report for the St. George Basin Planning Area Bering Sea, Alaska

OCS Report
MMS 87-0030

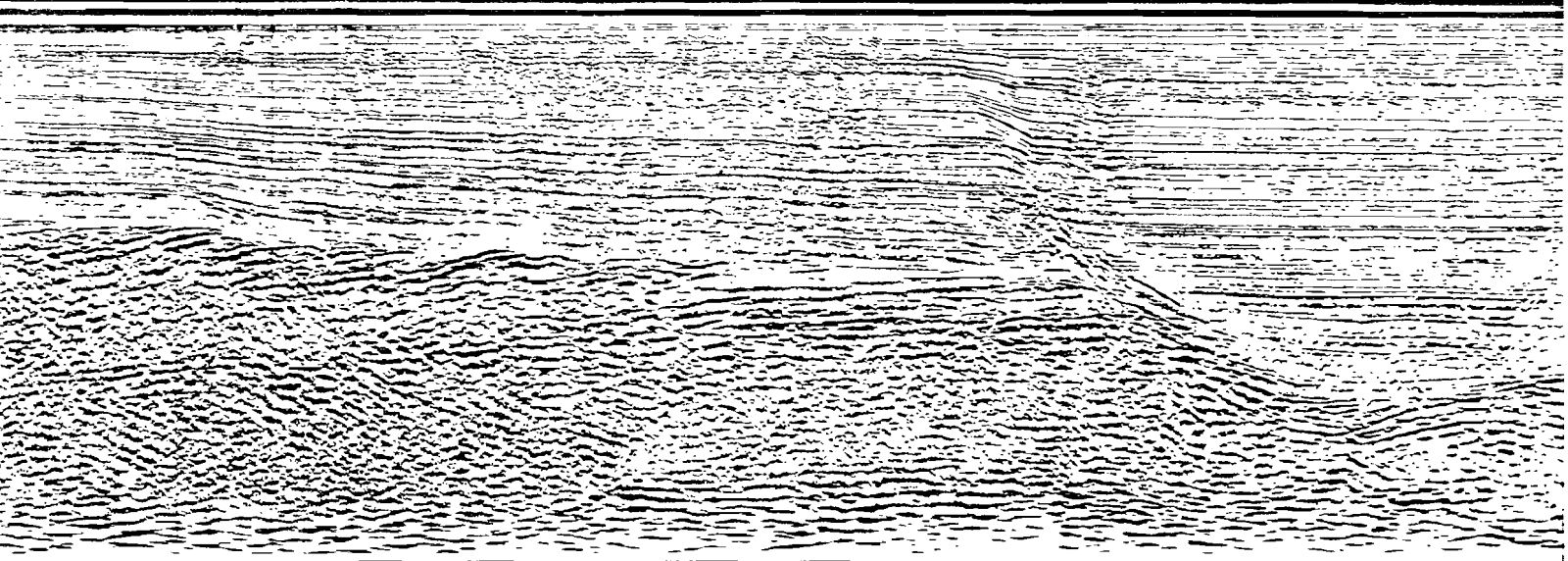

U.S. Department of the Interior
Minerals Management Service
Alaska Outer Continental Shelf Region

OCS Report
MMS 87-0030

Geologic Report for the St. George Basin Planning Area, Bering Sea, Alaska

by

C. DREW COMER
BRUCE M. HERMAN
SUSAN A. ZERWICK

1987

United States Department of the Interior
Minerals Management Service
Alaska OCS Region
Anchorage, Alaska

Contents

Figures

Tables

English-Metric Conversion

(The following table gives the factors used to convert English units to metric units.)

multiply English units	by	to obtain metric units
inches	2.5400	centimeters
feet	0.3048	meters
miles (statute)	1.6093	kilometers
square miles	2.5899	square kilometers
barrels (U.S. petroleum)	158.9828	liters
	0.1589	cubic meters

To convert from Fahrenheit (^{o}F) to Celsius (^{o}C), subtract 32 then divide by 1.8.

Geologic Report for the St. George Basin Planning Area, Bering Sea, Alaska

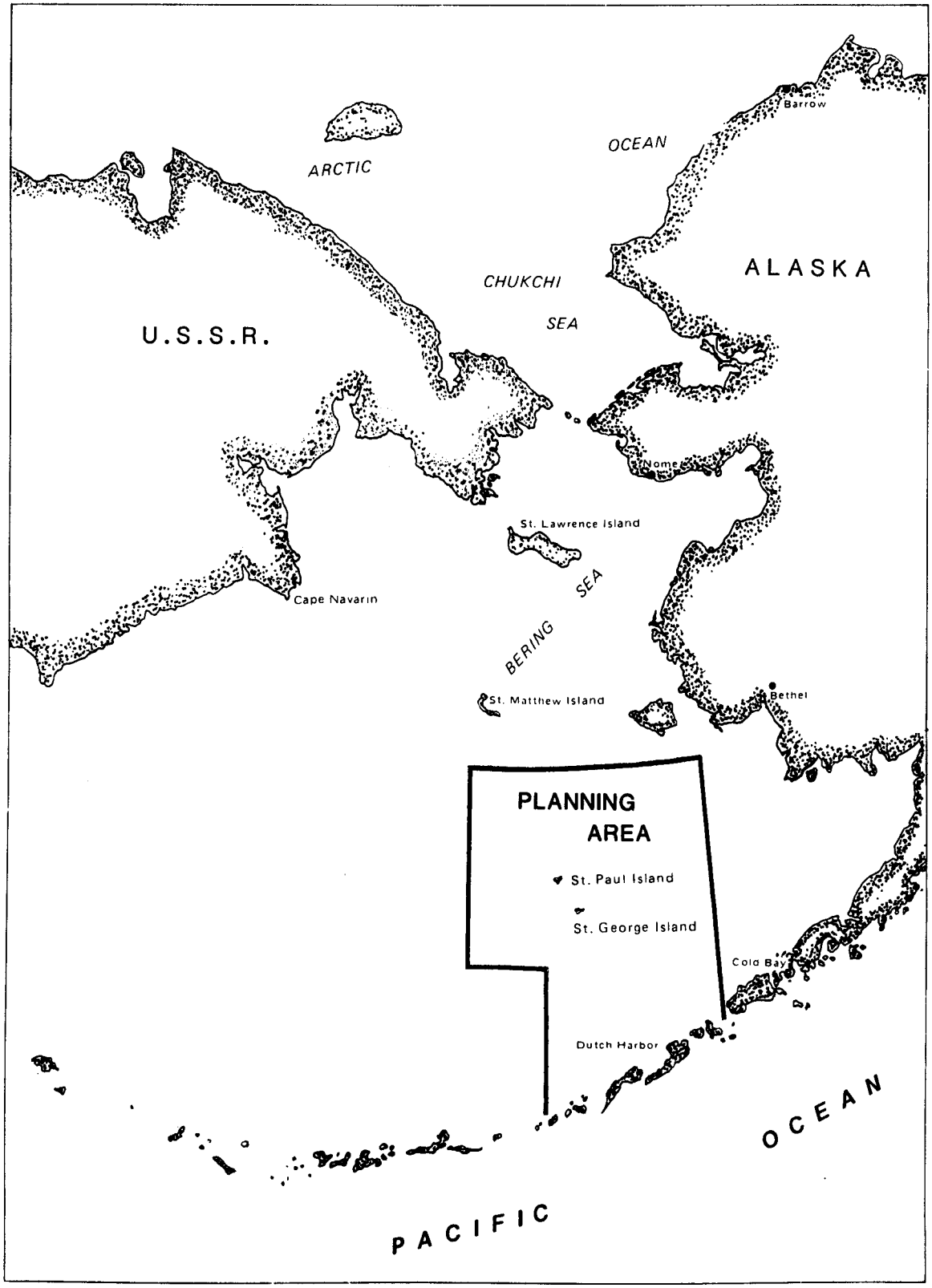

Figure 1. Location of the St. George Basin Planning Area.

Introduction

In September 1989, the Minerals Management Service (MMS) is scheduled to conduct Lease Sale 101 in the St. George Basin Outer Continental Shelf Planning Area. This report is a review of the geologic literature of the planning area and an interpretation of publicly available geological and geophysical data, particularly as they relate to potential hydrocarbon resources. Located in the Bering Sea, the St. George Basin Planning Area encompasses the southwestern portion of Alaska's outer continental shelf, slope, and rise (fig. 1). Of the 109,000 square miles in the planning area, the continental shelf comprises 73,000 square miles.

A contoured map of the bathymetry is shown in figure 2. The only prominent physiographic features on the shelf are the Pribilof Islands and the ridge upon which they sit. Except for some 3- to 6-foot fault scarps associated with the St. George graben, the shelf within the planning area is featureless (Comer, 1984a). The edge of the shelf is cut by two large submarine canyons, the Pribilof Canyon and the Bering Canyon. Bristol Canyon, a large submarine canyon on the slope and rise between the Bering and Pribilof Canyons, does not reach the shelf break. The Umnak Plateau, which may be uplifted oceanic crust (Cooper and others, 1980), is a major physiographic feature on the lower continental rise. The top of the plateau is slightly arched and is less than 2000 meters deep. The plateau is bounded on the east and north by the Bering Canyon and on the south by the Umnak Canyon.

Several major depocenters for Tertiary sediments are found within the planning area. On the shelf these include the St. George basin (Marlow and others, 1976) and the Pribilof basin (Scholl and Hopkins, 1969), which are shown in figure 3. The St. George basin is a graben 10 to 25 miles wide. The graben separates St. George Island and St. Paul Island, and extends approximately 200 miles to the southeast. Tertiary sediments within the graben reach a thickness of more than 40,000 feet. The Pribilof basin has a cross section similar to a half-graben, being bounded on its southwest side by a northwest-striking fault. This basin, which lies just landward of the shelf break and west of the Pribilof Canyon, is approximately 30 miles wide and 70 miles long. The maximum thickness of Tertiary sediments within the basin is 20,000 feet. Several other smaller basins, similar in structure to the Pribilof basin, underlie the Bering Sea shelf to the northwest (Cooper and

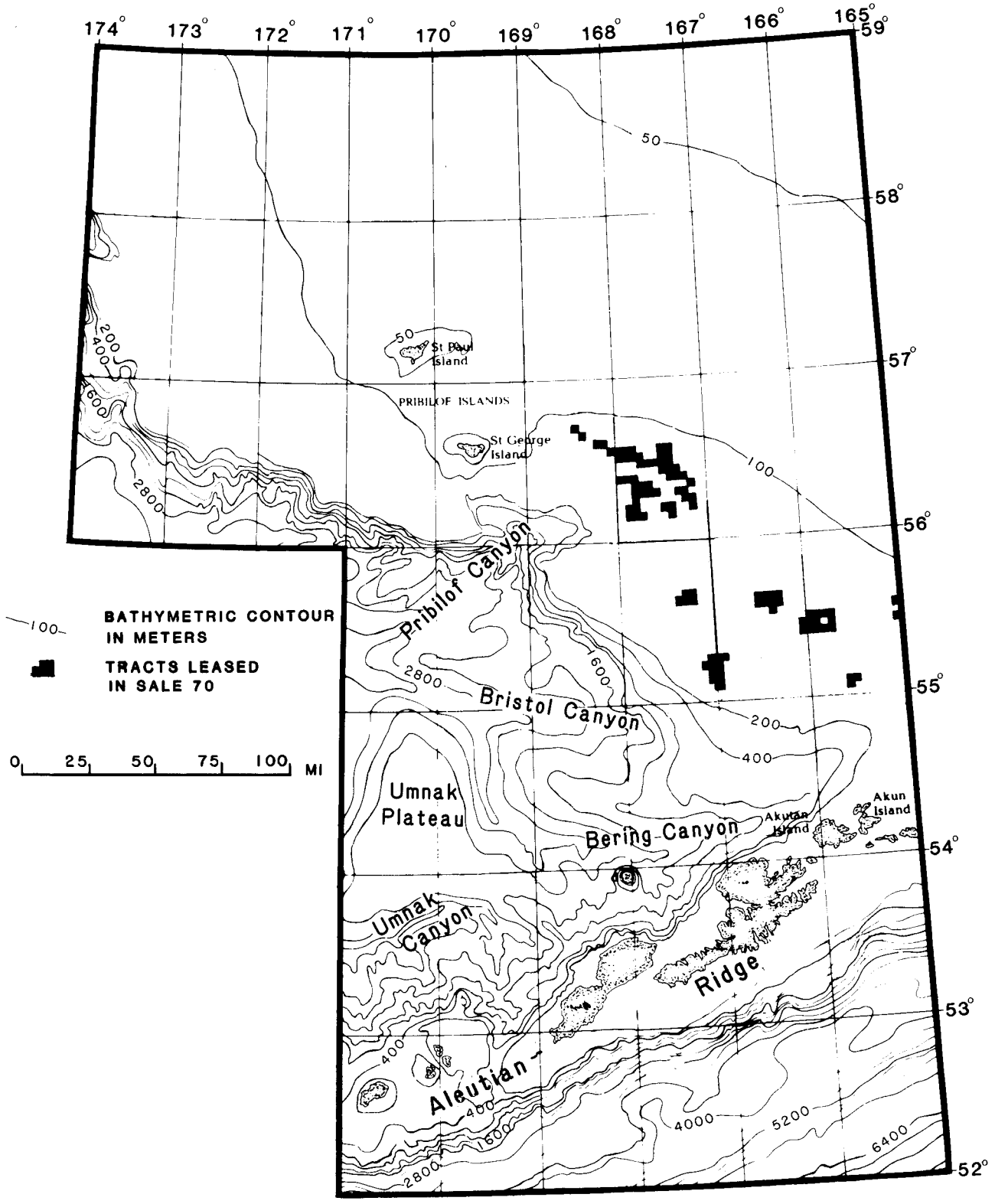

Figure 2. Bathymetric map of the St. George Basin Planning Area. Tracts leased in Sale 70 are darkened.

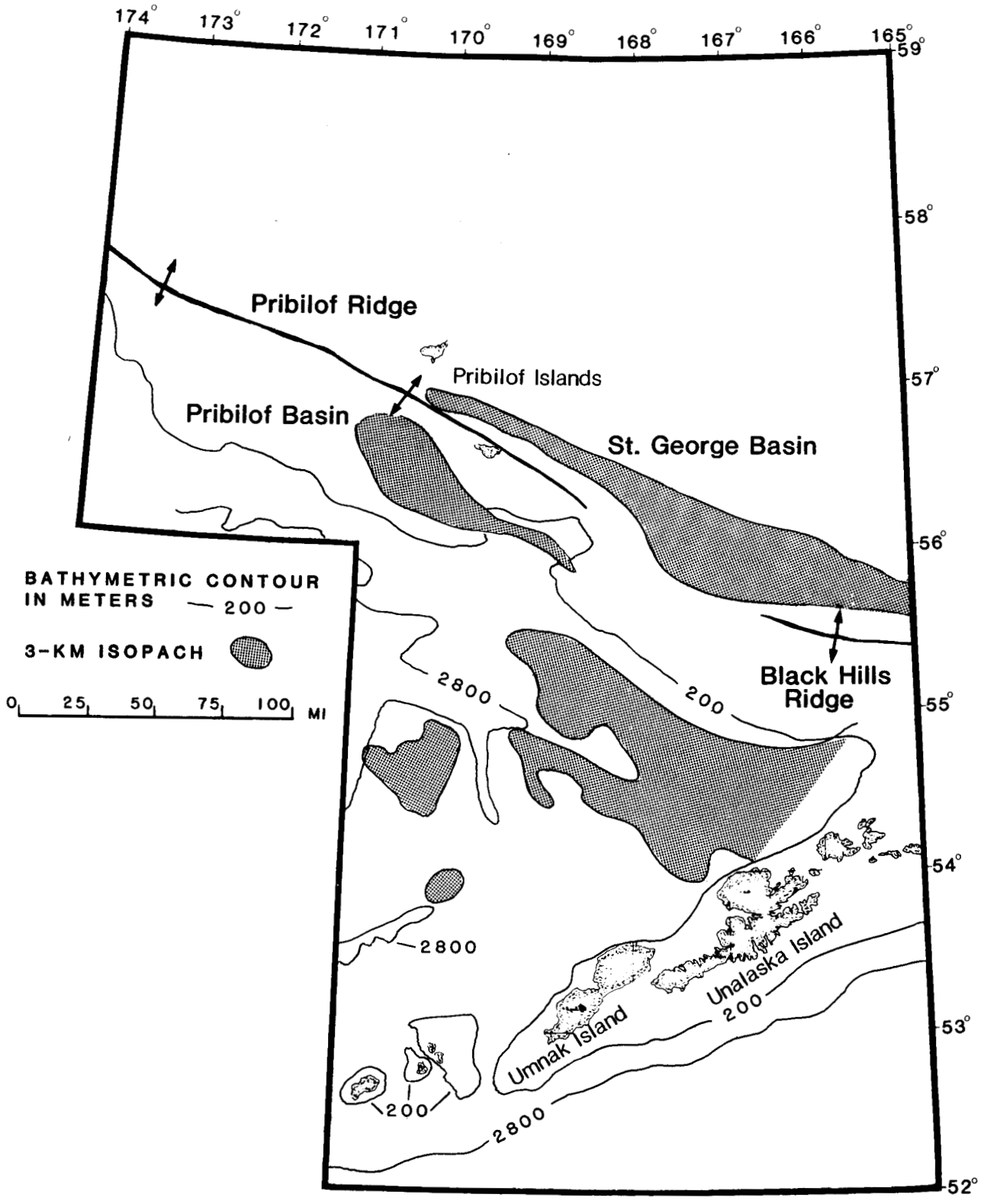

Figure 3. Simplified isopach map showing the major Tertiary depocenters in the St. George Basin Planning Area.

others, 1979a). As in the case of the Pribilof basin, none have any apparent sea-floor expression.

Seaward of the shelf edge, thick wedges of sediments have been identified beneath the Bering and Bristol Canyons (Cooper and others, 1979b), the Umnak Plateau (Scholl and others, 1968), and the continental rise (Cooper and others, 1984). The Bering and Bristol Canyons are underlain by sediments which reach thicknesses of more than 26,000 feet just north of the Aleutian Ridge. Sediments on the Umnak Plateau are generally greater than 6600 feet thick, and in two areas, totaling 115 square miles, they exceed 10,000 feet. Tertiary sediments beneath the continental slope and rise reach a thickness of 20,000 feet. These sediment accumulations differ markedly from the basins on the shelf in that they were not deposited in closed, subsiding basins.

To date, most of the exploration effort within the planning area has been concentrated in the St. George and Pribilof basins, because of their favorable water depths. Two Continental Offshore Stratigraphic Test (COST) wells and nine industry exploration wells have been drilled in the St. George Basin Planning Area, and a large quantity of multichannel seismic (MCS) reflection and sonobuoy refraction data has been acquired in both the St. George and Pribilof basins. Figure 4 is a trackline map of MCS reflection data acquired by Western Geophysical Corporation (WGC). Permission to use these data and the associated velocity data for this report, with some restrictions, was kindly granted by WGC. The locations of MCS lines used as illustrations in this report are shown in figure 5. Because of the data distribution and the low probability for economically recoverable petroleum resources in the deep-water areas of the planning area, the following discussion of the geologic history, petroleum geology, and environmental geology is essentially restricted to the St. George and Pribilof basins.

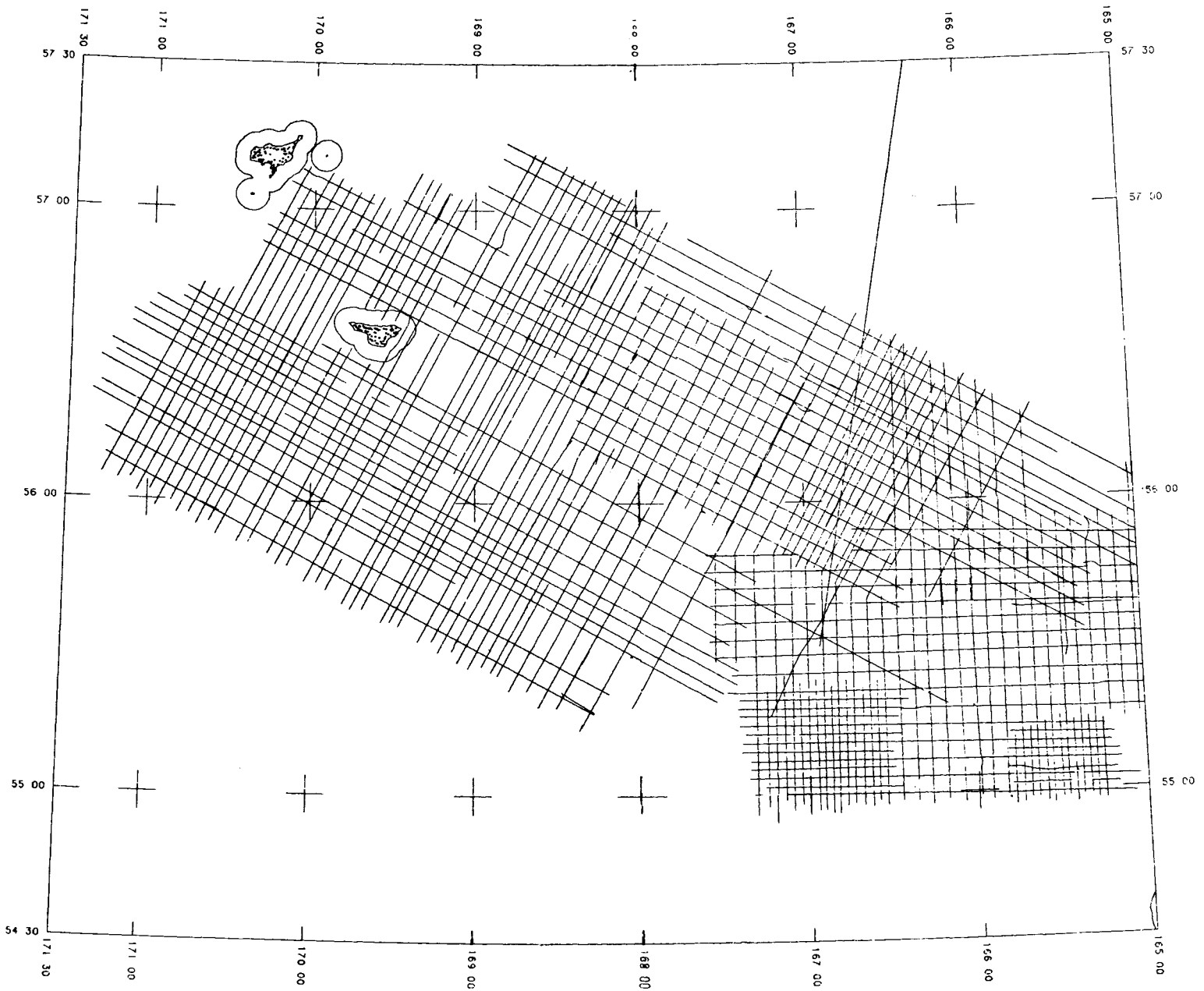

Figure 4. **Western Geophysical Company seismic lines used in mapping the St. George basin.**

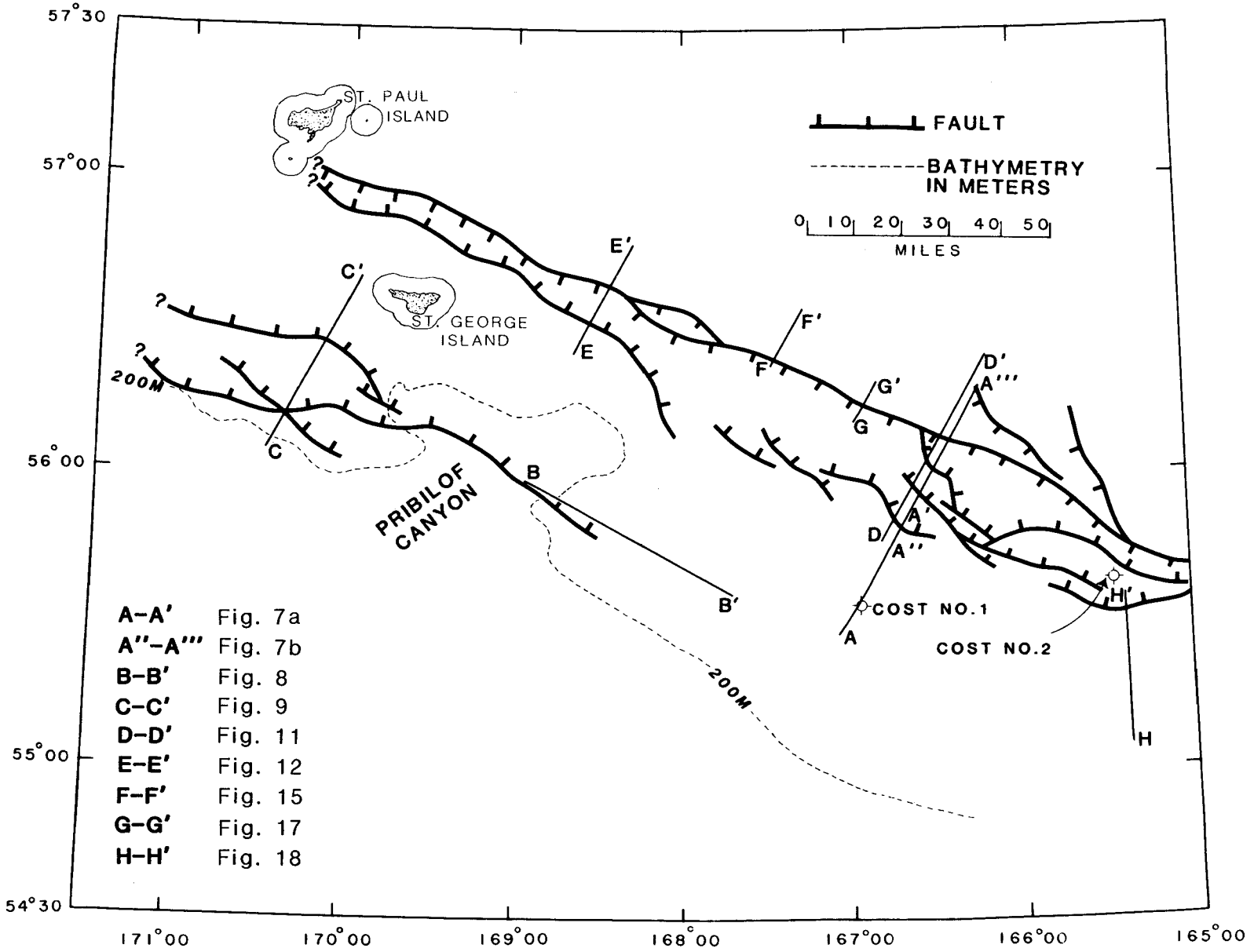

Figure 5. Western Geophysical Company seismic lines used as illustrations in this report.

1. Regional Geology

STRATIGRAPHY

Multichannel seismic reflection data from the St. George basin reveal an acoustically well stratified section overlying acoustic basement. Initially, the rocks of the acoustic basement were thought to be of Mesozoic age (Scholl and others, 1966, 1968), and those of the well-stratified sequence ("main layered sequence" of Scholl and others, 1968) were thought to be of Cenozoic age. The term acoustic basement is used loosely here, because coherent reflections are locally common beneath the top of the basement. We review here the stratigraphy of the St. George basin and the surrounding region, incorporating data released from the St. George basin COST wells (Bolm, 1984a, 1984b; Larson, 1984a, 1984b; AGAT Consultants, 1982) and interpretations drawn from a preliminary analysis of WGC velocity spectra. These data provide new constraints on the ages of the various sedimentary sequences in the St. George Basin Planning Area. Figures 6a and 6b summarize the stratigraphy of the two COST wells (Larson, 1984a, 1984b). Samples from the COST No. 2 well were provided by MMS to the Bujak Davies Group for a reexamination of the palynology. As a result, the biostratigraphy of that well has been somewhat revised from Larson (1984b) in the following discussion.

Mesozoic

The nearest exposures of Mesozoic rocks are on the Alaska Peninsula, where Burk (1965) described Upper Jurassic (Oxfordian and Kimmeridgian) siltstones and sandstones of the Naknek Formation in the Black Hills and at Herendeen Bay. Overlying the Naknek are the Upper Jurassic and Lower Cretaceous Staniukovich Formation, the Lower Cretaceous Herendeen Limestone, and the Upper Cretaceous Chignik, Hoodoo, and Kaguyak Formations (Detterman, 1982). The Staniukovich and Chignik Formations consist of shallow marine siltstones and sandstones. The Hoodoo Formation is composed of outer neritic to deep marine siltstones, silty shales, and claystones with fine-grained sandstones. With the exception of an unnamed sequence of Albian rocks in the northern part of the peninsula, rocks of Barremian through Santonian age are absent. A serpentinized peridotite on St. George Island is also thought to be of Mesozoic age, based on a 50 to 57 million year (m.y.) radiometric age obtained from a granodiorite dike which intrudes the peridotite (Hopkins and Silberman, 1978).

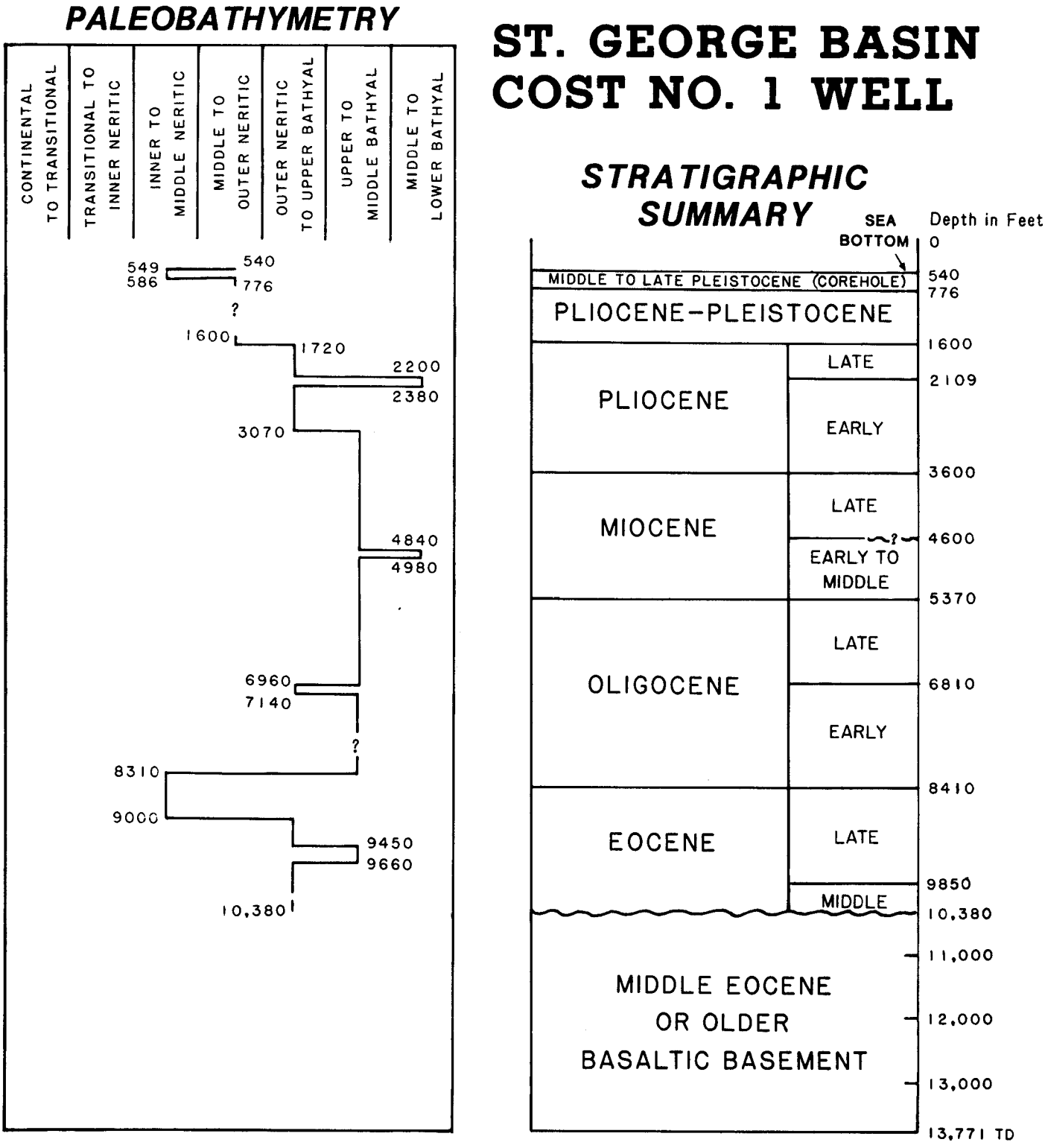

Figure 6A. Stratigraphic summary and paleobathymetry for the St. George COST No. 1 well (modified from Larson, 1984a).

ST. GEORGE BASIN COST NO. 2 WELL

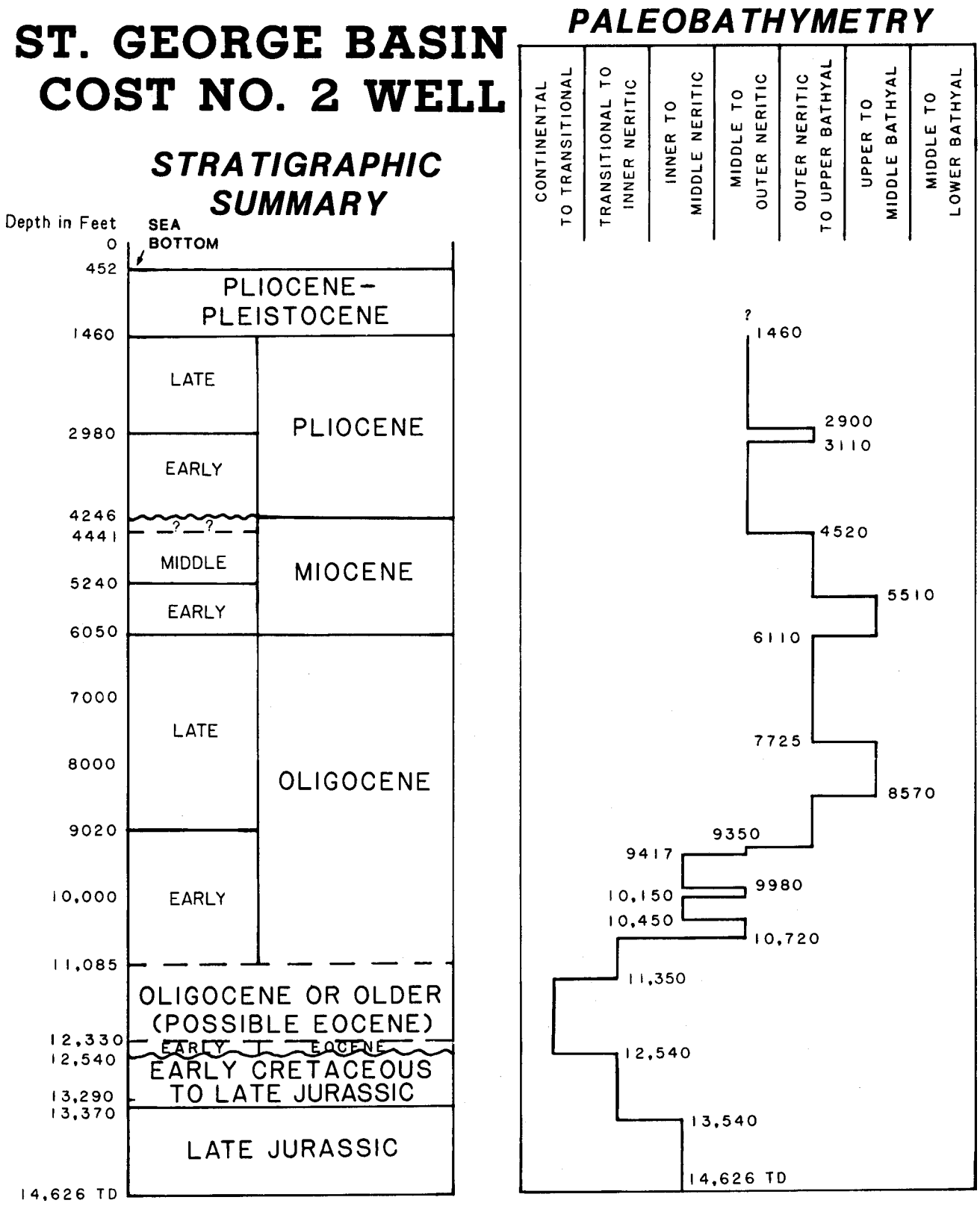

Figure 6B. Stratigraphic summary and paleobathymetry for the St. George COST No. 2 well (modified from Larson, 1984b).

The Pribilof ridge is a basement high that separates the Pribilof basin from the St. George graben. Vallier and others (1980) dredged submarine outcrops of the Pribilof ridge approximately 15 miles east of St. George Island and recovered Upper Jurassic siltstones and volcanic sandstones. McLean (1979) and Vallier and others (1980) believe these rocks are equivalent to the Naknek Formation, based on the presence of the pelycypod Buchia of Jurassic (Kimmeridgian) age and the presence of green hornblende, which is a common accessory mineral in Naknek rocks on the Alaska Peninsula.

Upper Jurassic (Oxfordian and Kimmeridgian) sandstones, siltstones, and conglomerates were recovered in the bottom of the St. George COST No. 2 well (Larson, 1984b). Lithic fragments in the siltstones and sandstones are primarily volcanic. The conglomerates contain large volcanic clasts, which suggests a nearby source. We believe that these marine shelf sediments are equivalent to the Naknek Formation.

Naknek rocks from the Alaska Peninsula are arkosic and were derived from a plutonic terrane (Vallier and others, 1980), whereas the coeval rocks from the Pribilof ridge and the St. George COST No. 2 well were derived from a volcanic terrane. Vallier and others (1980) proposed that the Naknek rocks from the Alaska Peninsula and equivalent rocks from Pribilof ridge were derived from a magmatic arc that Reed and Lanphere (1973) believed extended along the Beringian continental margin during the Jurassic. The difference in source terranes resulted from differential uplift of the arc. Uplift of the arc near the Alaska Peninsula by the Late Jurassic was sufficient to allow the volcanic arc to be completely unroofed. Plutonic rocks were thus exposed and became the source for Naknek sediments. Uplift at the present-day Bering shelf was insufficient to expose plutonic rocks, and only volcanic rocks were available in the source terrane for Late Jurassic sediments. We believe that this scenario can be extended into the Cenozoic, because plutonic rocks do not constitute a significant portion of the lithic fragments in either the Mesozoic or Cenozoic rocks in the St. George basin, indicating that the volcanic arc was never completely unroofed on the shelf.

Upper Jurassic to Lower Cretaceous sandstones, conglomerates, and siltstones, with minor shale and coal, overlie the Naknek-equivalent rocks at the COST No. 2 well. These rocks were deposited in a fluvial to deltaic and possible inner neritic environment. Both metamorphic and volcanic rock fragments occur in the sandstones; volcanic and sedimentary clasts occur in the conglomerates (Bolm, 1984a). These rocks may be equivalent to the Staniukovich Formation (Portlandian and Neocomian), which overlies the Naknek Formation on the Alaska Peninsula. However, the upper 750 feet of the Upper Jurassic to Lower Cretaceous section at the COST No. 2 well may actually be Paleocene based on palynology (J. Bujak, written commun., 1986).

Upper Cretaceous rocks were not present at the COST No. 2 well. An unconformity separates the Upper Jurassic to Lower Cretaceous sequence from the overlying Tertiary section. Upper Cretaceous

sandstones and siltstones were recovered, however, in dredge hauls from Pribilof Canyon (Scholl and others, 1966; Hopkins and others, 1969). McLean (1979) suggested that these Upper Cretaceous rocks may be correlative with the Hoodoo Formation on the Alaska Peninsula.

Cenozoic

In the vicinity of the planning area, the oldest exposed Tertiary section is the Tolstoi Formation, which crops out on the Alaska Peninsula (Burk, 1965; Brockway and others, 1975). The Tolstoi Formation unconformably overlies the Mesozoic section and contains Paleocene through Eocene siltstones with interbedded volcanic sandstones. These rocks were deposited in a nonmarine to brackish-water environment. Basalt flows and sills are also found in the Tolstoi Formation. Another occurrence of Eocene age rocks is on St. George Island, where a 50 to 57 m.y. granodiorite dike intrudes ultramafic rocks of unknown age (Hopkins and Silberman, 1978).

At the St. George COST No. 1 well, the deepest rocks penetrated were basalts and tuffs (10,380 to 13,771 feet). Potassium-argon age dates from the basalts range from 23 to 136 m.y., but these data are not believed to be reliable (Bolm, 1984b). The wide range of ages is most likely caused by the highly altered state of the basalts. Although the age of the basalts is indeterminate, we tentatively assign a Paleocene to early Eocene age to them.

An unconformity separates a middle Eocene basal conglomerate from the basalts at the well and corresponds to the seismically observed unconformity between the main layered sequence (Cenozoic) and acoustic basement (Mesozoic), which were identified and dated by Scholl and others (1966, 1968). The age assigned by Scholl and others to the unconformity was based on the similarity of this unconformity to the unconformity that separates the early Tertiary Tolstoi Formation from the Late Cretaceous Chignik and Hoodoo Formations onshore (Scholl and others, 1966, 1968). Marlow and Cooper (1980) observed that the seismic unconformity could be traced over a layered sequence within the Bristol Bay basin (here called North Aleutian basin). Those investigators tentatively assigned a Mesozoic age to the layered sequence below the unconformity. This seismically identifiable surface is shown in figure 7a, which is a seismic line tied to the COST No. 1 well, and is labeled ABU for acoustic basement unconformity.

As mentioned above, coherent seismic reflections commonly occur below the acoustic basement surface. In some areas, coherent reflections are observed as much as 4 seconds below the ABU. Within the upper half to one second of section (two-way travel time) below the ABU, interval velocities may be as low as 11,000 feet/second. Velocities such as this are comparable to the velocities of lower Tertiary sedimentary rocks at the COST No. 1 well. On this basis we speculate that at least in some areas the upper portion of the section previously identified as Mesozoic consists of lower Tertiary strata. According to Larson (1984b), the ABU separates Mesozoic and Cenozoic strata at the COST No. 2 well, but based on palynology

(J. Bujak, written commun., 1986), the ABU may separate Paleocene and lower Eocene strata at the COST No. 2 well. In either case, we do not believe that the ABU is a Mesozoic-Cenozoic boundary throughout the Bering shelf. The ABU surface is most likely time transgressive and does not represent a single erosional event or a simple time boundary. The results of the velocity analyses and other data that relate to the ABU are discussed in the Acoustic Basement section of this report.

The basal conglomerate that unconformably overlies the basalts at the COST No. 1 well contains volcanic clasts that were derived from the underlying basalt. This basal conglomerate and the overlying siltstones and sandstones range in age from middle to late Eocene, and are thought to have been deposited in a marine shelf environment (Larson, 1984a). No basal conglomerate was reported in the St. George COST No. 2 well. The oldest Tertiary rocks at the COST No. 2 well, from 11,085 to 12,540 feet, could only be dated as Oligocene or older by Larson (1984b) because of the paucity of fossils. However, according to J. Bujak (written commun., 1986), palynological data indicate an early Eocene age for the base of this section beginning at 12,330 feet. The basal Tertiary sediments in the COST No. 2 well are composed of sandstones, siltstones, and mudstones that were deposited in a nearshore or nonmarine environment.

During the Oligocene the depositional environment in the St. George basin became more marine, possibly because of rapid shelf subsidence (figs. 6a and 6b). The depositional environment at the COST No. 1 well changed from nearshore to upper bathyal in the earliest Oligocene time. At the COST No. 2 well the environment changed from continental or transitional to upper bathyal in the Oligocene. Interbedded sandstones, siltstones, and mudstones were deposited during the Oligocene at both COST well sites. Volcanic lithic fragments predominate in these rocks in the COST No. 1 well. In the COST No. 2 well metamorphic as well as volcanic lithic fragments are common.

At the COST No. 1 well a pebbly sandstone grading downward into a conglomerate was reported from 7600 to 7860 feet within the latest early Oligocene (Bolm, 1984a). The conglomerate corresponds to a seismically defined horizon, labeled II in figure 7a, that is conformable within local basement depressions and truncates acoustic basement highs near the well (fig. 7a). No conglomerate was found in coeval rocks in the COST No. 2 well.

An unconformity (horizon I, fig. 8) is apparent on seismic profiles in the upper Oligocene section near the shelf edge. It can be traced into the Pribilof basin, where it is an angular unconformity (fig. 9). In the Pribilof basin horizon I truncates relatively disrupted and incoherent seismic reflections. We interpret these disrupted reflections below the unconformity to represent coarse detritus deposited in a nonmarine environment during an early phase of basin subsidence. Pribilof ridge and the basement ridge which bounds the Pribilof basin on the south were probably

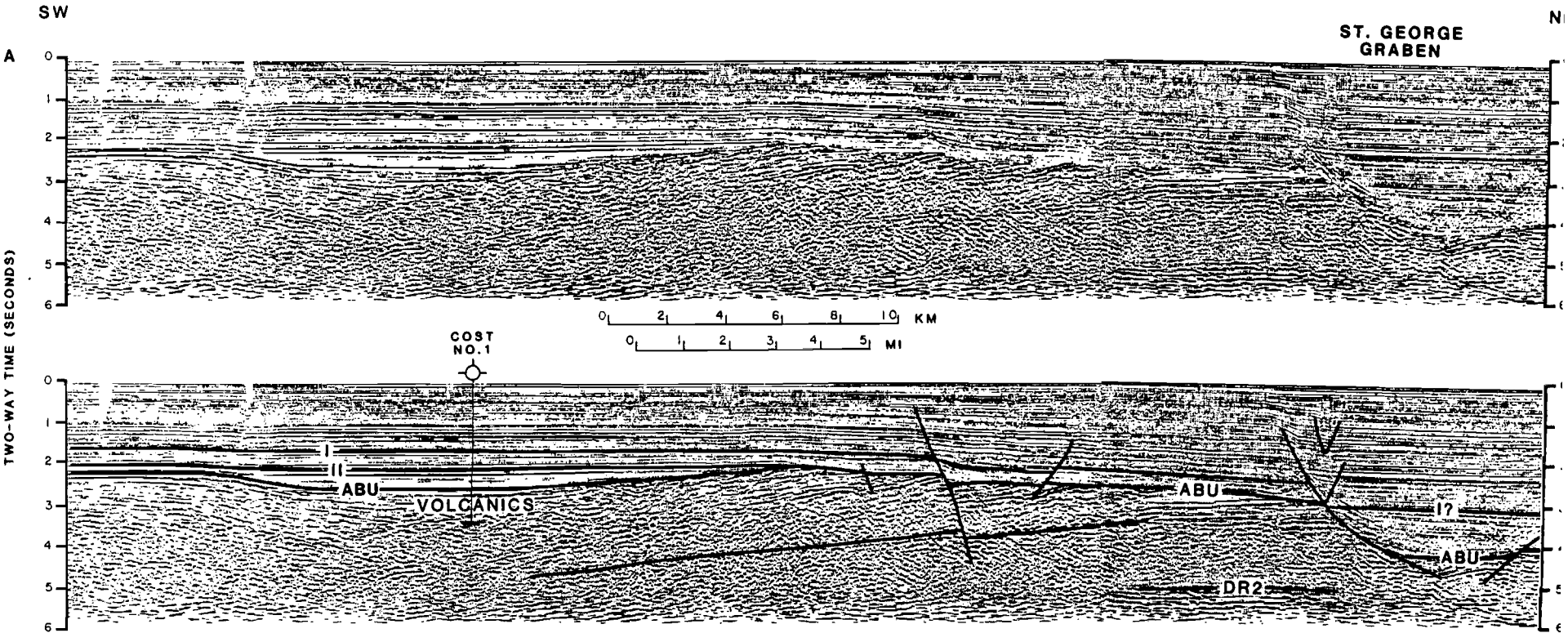

Figure 7A. A-A': Migrated seismic profile (courtesy of Western Geophysical Company) near the COST No. 1 well. Horizon I occurs near the top of an upper Oligocene sandstone sequence in the well and has been tentatively correlated into the St. George graben. Horizon II is a lower Oligocene conglomeratic sandstone that truncates against the acoustic basement unconformity (ABU). The ABU is a time-transgressive, angular unconformity that is middle Eocene or older at the COST No. 1 well and early Eocene or older at the COST No. 2 well.

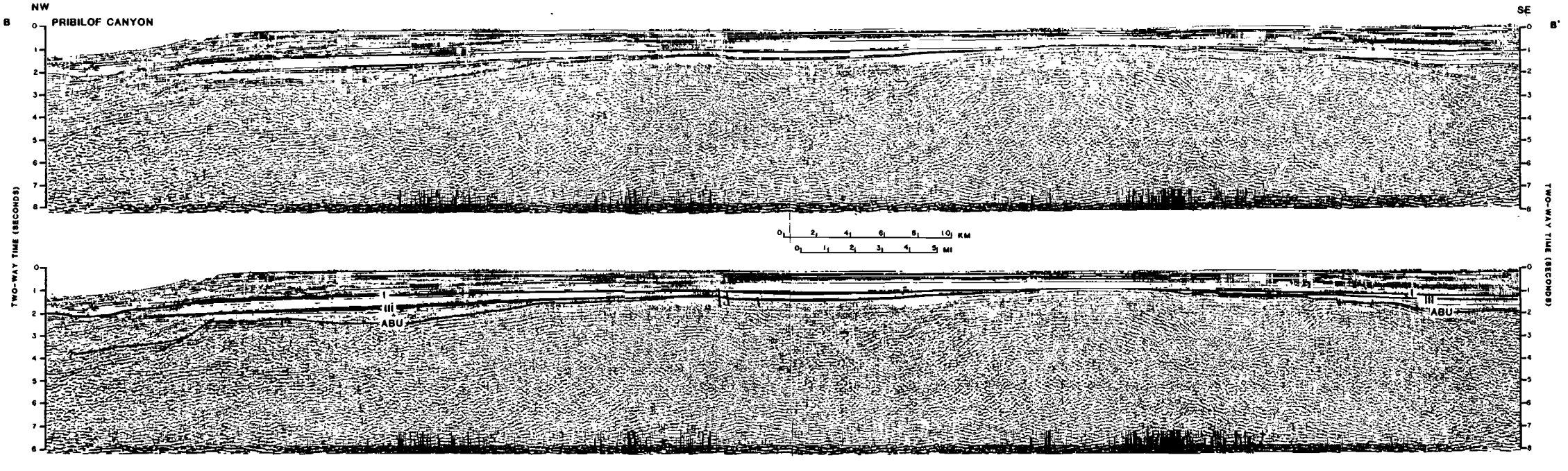

Figure 6. B–B': Migrated seismic profile (courtesy of Western Geophysical Company) showing an upper Oligocene unconformity, horizon I, near the shelf edge. Horizon I can be traced into the COST No. 1 well (fig. 7a), where it is apparently conformable, and into the Pribilof basin (fig. 9), where it is an angular unconformity. Horizon III is a probable Oligocene unconformity.

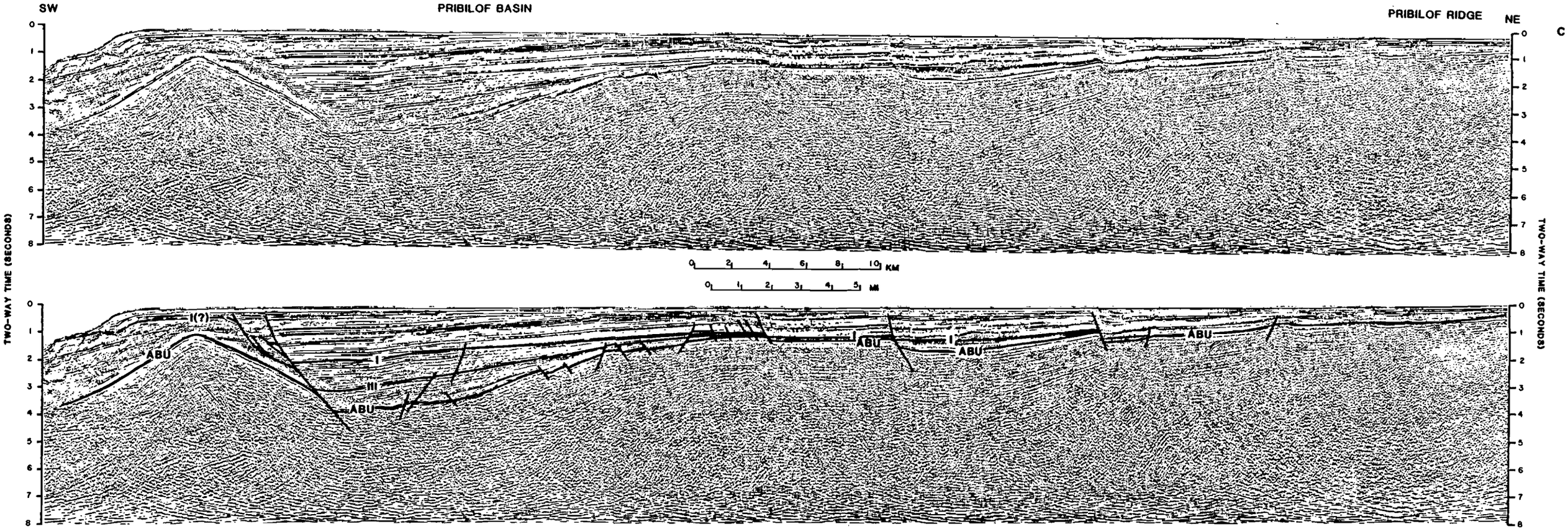

Figure 9. C–C': Migrated seismic profile (courtesy of Western Geophysical Company) illustrating the half-graben appearance of Pribilof basin. Horizon I is an upper Oligocene angular unconformity which truncates against Pribilof ridge. Horizon III is a probable Oligocene unconformity which is truncated by horizon I.

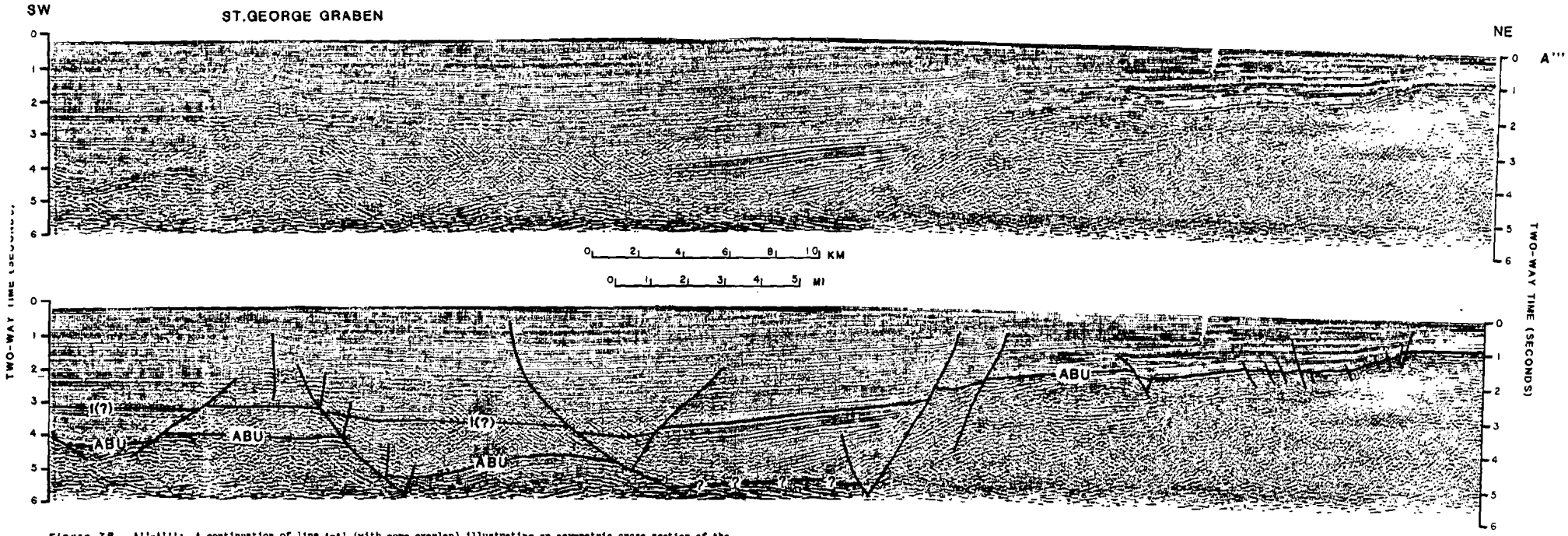

Figure 7B. A''-A''': A continuation of line A-A' (with some overlap) illustrating an asymmetric cross section of the St. George graben. Horizon I(?) is mapped on high-amplitude, low-frequency reflections south of the northern boundary fault of the graben. These reflections are thought to represent a coarse clastic sequence.

sources for these clastic sediments. Strata overlying the unconformity are acoustically well stratified and are interpreted to be marine shelf sediments. The unconformity truncates Pribilof ridge (fig. 9). Landward from the shelf edge and Pribilof ridge, horizon I is either a disconformity or it becomes conformable. No hiatus is observed in paleontologic data from the COST No. 1 well (fig. 7a). It is interesting to note that horizon I correlates with the top of an Oligocene sand that is mappable across much of the planning area.

Miocene samples recovered from both COST wells indicate an outer neritic to upper bathyal depositional environment. Miocene sediments consist of mudstones, siltstones, and sandstones. Lithic fragments at the COST No. 1 well are predominantly volcanic, whereas those at the COST No. 2 well are both volcanic and metamorphic.

A disconformity in the late Miocene section is indicated at 4600 feet in the COST No. 1 well (fig. 6a) and at 4246 feet in the COST No. 2 well (fig. 6b). Below this apparent disconformity, siliceous microfossils are absent in the COST No. 1 well and are only poorly preserved in the COST No. 2 well (Larson, 1984a, 1984b). In both wells, an increase in density and sonic velocity is also recorded on wireline logs at these depths (see plates 1, Turner and others, 1984a, 1984b). Although these data are consistent with a disconformity, the lack of a seismic reflection tying the disconformity between the two wells is sufficiently contradictory to preclude a basin-wide depositional hiatus. The observed changes in the physical properties of the sediments suggest a phase transformation.

Bottom simulating reflectors (BSR's) are common on the Bering Sea shelf, including St. George basin, and are usually interpreted as being seismic reflections from the acoustic impedance change that accompanies the transition with depth of opal-A to opal-CT (Hammond and Gaither, 1983). Turner and others (1984c), however, found very little opal-CT in the Navarin Basin COST well below the depth at which a BSR would be expected. Iijima (1980) and Iijima and Utada (1983) observed that in the presence of volcaniclastic sediment, opal-A transformed into clinoptilolite rather than opal-CT. Turner and others (1984c) concluded that the transformation reported by Iijima (1980) and Iijima and Utada (1983) was the most likely cause of the BSR in Navarin Basin, because this basin is filled with volcaniclastic sediment and clinoptilolite was found in the Navarin Basin COST well below the depth at which a BSR would be expected. St. George basin is also filled with volcaniclastic sediment, and clinoptilolite was reported as an authigenic mineral in cores from the COST No. 2 well below 5000 feet (Bolm, 1984b). Following Turner and others (1984c), we therefore believe the disappearance of the siliceous microfossils to be the result of a phase transformation of biogenic opal-A to clinoptilolite.

Pliocene strata at the COST No. 1 well are made up of sandstone, siltstone, and mudstone. At the COST No. 2 well, the correlative strata are primarily diatomaceous mudstones with lesser amounts of siltstone, sandstone, and minor conglomerate. The lithic component

of the sediment at both well sites consists of volcanic fragments. Paleoenvironments at the COST No. 1 well become more shallow throughout the Pliocene, going from upper bathyal to middle neritic. In the COST No. 2 well the paleoenvironments are generally middle to outer neritic throughout this time. A brief deepening trend occurs at the top of the lower Pliocene in both wells (Larson, 1984a, 1984b).

STRUCTURAL SETTING

The main structural feature in the planning area is the St. George graben. The graben separates St. Paul Island and St. George Island, and extends southeastward into the North Aleutian Basin Planning Area. As the graben crosses from the St. George Basin Planning Area into the North Aleutian Basin Planning Area, its strike becomes more easterly. Figure 10 is a structure-contour map of the acoustic basement surface and shows the fault patterns on the shelf.

The graben is filled with Tertiary strata that are generally well stratified acoustically. These strata overlie Upper Jurassic rocks at the site of the Exxon well (Y-0530) and Lower Cretaceous to Upper Jurassic rocks at the COST No. 2 well. The Tertiary sediments, which were deposited syntectonically with the subsidence of the graben, frequently exhibit drag along faults within the graben, whereas older rocks appear to break in a brittle fashion. This configuration indicates that the graben is at least post-Early Cretaceous in age. Subsidence has continued through recent times, as is demonstrated by sea-floor fault scarps up to 6 feet high (Comer, 1984a). These surface faults are continuations of the faults seen at depth offsetting Tertiary and Mesozoic strata.

The faults that bound the graben are basement-controlled growth faults. Dip along the faults decreases with depth, but the fault planes do not sole out within the 8 seconds of two-way travel time recorded on the MCS reflection records (figs. 7a, 7b, and 11). A paucity of rotated fault blocks within the graben is further evidence that the dip of fault planes does not decrease substantially with depth. For instance, figures 7a and 7b illustrate a typical profile across the graben. Only one of the large fault blocks exhibits noticeable rotation, approximately 15° in this case. Several smaller rotated fault blocks are apparent in figure 11, but the major blocks do not appear to have been rotated.

The St. George graben is asymmetric in two respects. First, the northern boundary fault is continuous along nearly the entire length of the graben within the planning area, whereas discontinuous, en echelon faults occur along the southern border (fig. 10). Second, the magnitude of fault displacement is consistently greatest along the northern side of the graben. Indeed, the entire vertical offset along the northern side frequently occurs across a single fault, where the offset can be as much as 30,000 feet. Offset along the southern margin occurs across several faults and over a much broader

area. The degree of asymmetry varies from highly asymmetric (figs. 7a, 7b, and 11) to only slightly asymmetric (fig. 12). The continuity of the northern boundary fault, the consistent asymmetry of the profile of the graben, and the magnitude of the offset along the northern boundary fault suggest that this fault is a major discontinuity in the earth's crust.

Splays from the northern bounding fault become common as the graben passes from the St. George Basin Planning Area into the North Aleutian Basin Planning Area near 165° W longitude. Mapping in the North Aleutian Basin Planning Area has revealed that the southern faults of the St. George graben coalesce eastward into a major strike-slip fault. This geometry suggests that the St. George graben opened as a rhombochasm in a right-lateral strike-slip fault system in which the plane of slip was stepping to the north. A second implication of this geometry is that the northern boundary fault in the St. George Basin Planning Area may have a significant component of horizontal offset in addition to vertical offset.

The acoustic basement highs on the southern flank of the St. George graben form a discontinuous ridge that extends from the Black Hills on the Alaska Peninsula to the Pribilof ridge, on which St. George Island sits. This ridge has been informally named the Black Hills ridge (Marlow and others, 1976). Onshore, the Black Hills are cored by Mesozoic rocks of the Naknek Formation (Burk, 1965). Sampling offshore is limited to the downfaulted northern flank of the ridge where the COST No. 2 well cored possible Paleocene rocks and Mesozoic rocks ranging in age from Late Jurassic through Early Cretaceous. The Black Hills ridge is associated with a linear magnetic trough, discussed in more detail in the Acoustic Basement section.

Reflections from strata within the acoustic basement in the St. George Basin Planning Area vary from relatively weak and discontinuous to strong and laterally extensive. Coherent reflections can be seen in places to depths as great as 30,000 feet. South of the graben, where the deepest reflections are visible, reflections tend to be flat lying or dipping slightly to the south (fig. 7a). Shallower subbasement reflections are folded into broad, northwest-trending, faulted synforms. These synforms can be traced for as much as 30 miles. As noted above, the upper 0.5 to 1.0 second of the subbasement section appears to be early Tertiary in places. Folds in these strata indicate compressional tectonics during that time. Subbasement reflections to the north of the graben are not as continuous as those to the south.

Pribilof basin underlies the shelf south of the St. George graben, near the shelf edge. Figure 9 shows a Western Geophysical Company MCS line across the Pribilof basin. The Pribilof basin differs substantially from the St. George graben in that subsidence in the basin was fault controlled on only its southwest side, giving a half-graben appearance. The basin-bounding faults are basement controlled and mildly listric. The dip-slip component of fault movement was normal, with the downthrown side to the northeast.

Faulting occurred contemporaneously with deposition. Strata in the basin thin to the northeast as they rise over Pribilof ridge and are truncated near the sea floor. A shelf-edge ridge, which parallels Pribilof ridge, is present to the southwest of the basin-bounding fault (fig. 9).

The asymmetric Pribilof basin is similar in structural style to the basins of the California continental borderland described by Howell and others (1980). These basins are believed to have been formed in response to strike-slip motion between the Pacific and North American plates. The similarity of styles, together with the tectonic history of the Beringian margin, suggests that strike-slip motion was a major component of fault movement on the southwest side of the Pribilof basin.

The eastern end of Pribilof basin is breached by the Pribilof Canyon (fig. 10). The border fault and the shelf-edge ridge south of the basin extend into the canyon. The canyon is "T" shaped, with one axis perpendicular to and one axis parallel to the shelf edge. The border fault coincides with one of the canyon walls parallel to the shelf edge. This geometry suggests that structural control played a major role in canyon development. A large volume of Tertiary sediment has been removed by headward erosion of the canyon. The canyon has also carved into Mesozoic rocks beneath the acoustic basement unconformity, as evidenced by Upper Cretaceous sedimentary rocks dredged from the canyon by Hopkins and others (1969).

The Umnak Plateau lies south of the Pribilof basin and beyond the shelf edge. The Umnak Plateau rises roughly 1200 meters above the Aleutian Basin near the junction of the Aleutian Ridge and the Bering shelf (fig. 2). The plateau, which was first described by Scholl and others (1968), is covered by sediments that in places are greater than 3 kilometers thick (Cooper and others, 1980). Seismic refraction data indicate that the strata on the Umnak Plateau overlie what appears to be uplifted oceanic crust (Cooper and others, 1980). The strata on the plateau are undeformed, except locally where they are faulted or gently folded. These faults do not reach the sea floor (Cooper and others, 1980), and much of the folding is associated with shale diapirs which rise from depths near acoustic basement (Scholl and Marlow, 1970). The diapirs, which occur both individually and in groups, have structural reliefs ranging from 500 to 1500 meters. Childs and others (1979) proposed that the source of the shale is a 0.3-second-thick (two-way travel time) interval that lies between the top of the acoustic basement and the top of the oceanic crust.

To the east of the Umnak Plateau and beneath the Bering and Bristol Canyons (fig. 2) lies a major sediment depocenter that was described by Cooper and others (1980). In this area the acoustic basement dips toward the Aleutian Ridge, as do the overlying strata. The thickness of these strata increases to the south, exceeding 8 kilometers near the Aleutian Ridge. The strata do not appear to have been tectonically deformed.

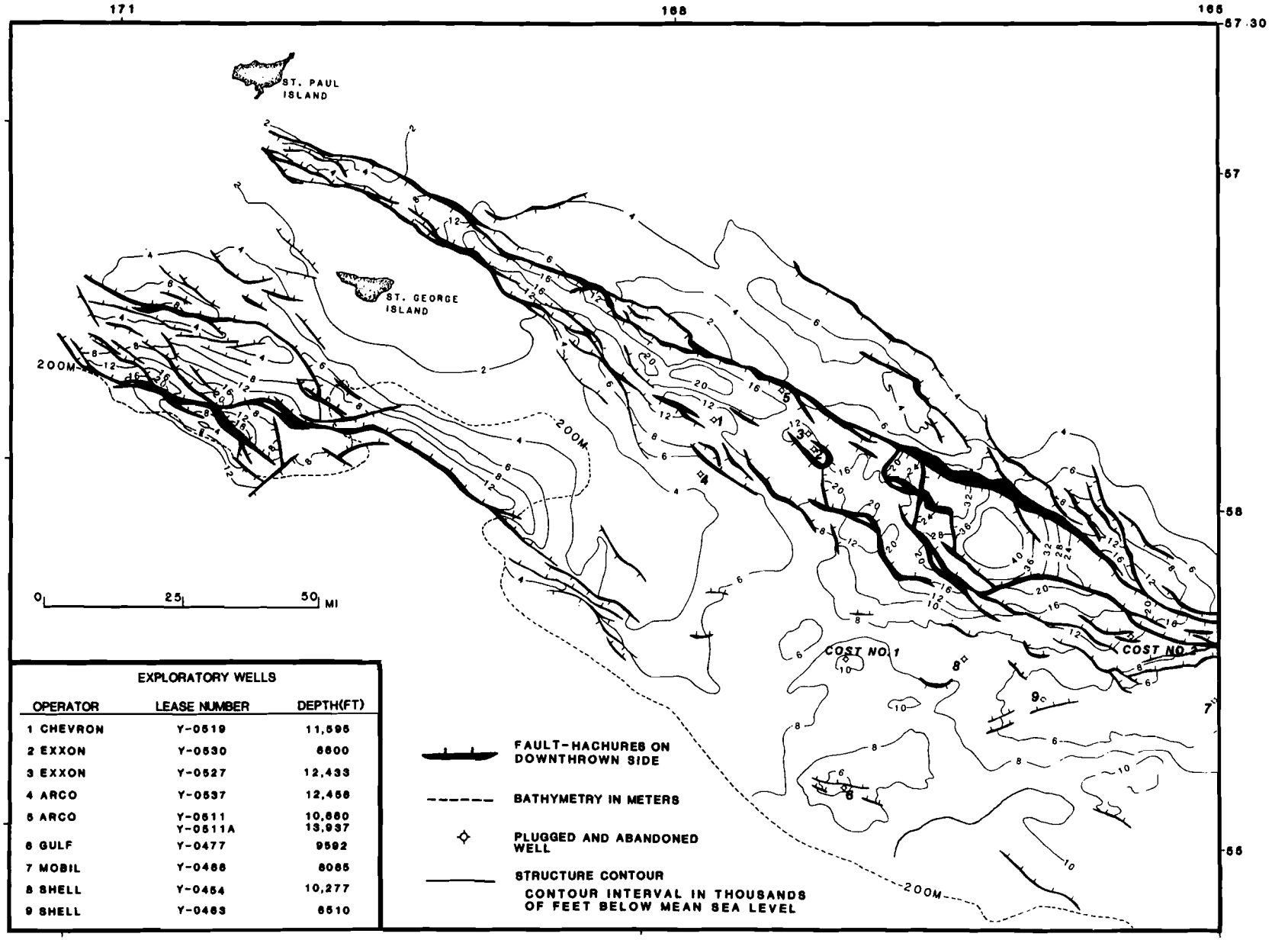

EXPLORATORY WELLS

OPERATOR	LEASE NUMBER	DEPTH(FT)
1 CHEVRON	Y-0519	11,595
2 EXXON	Y-0530	6600
3 EXXON	Y-0527	12,433
4 ARCO	Y-0537	12,456
5 ARCO	Y-0511 Y-0511A	10,660 13,937
6 GULF	Y-0477	9592
7 MOBIL	Y-0486	8085
8 SHELL	Y-0454	10,277
9 SHELL	Y-0463	6510

Figure 10. Structure-contour map of the acoustic basement unconformity (ABU) in the St. George Basin Planning Area. Contour lines are labeled in thousands of feet below mean sea level. Contour interval is 4000 feet in the St. George graben and Pribilof basin, and 2000 feet elsewhere.

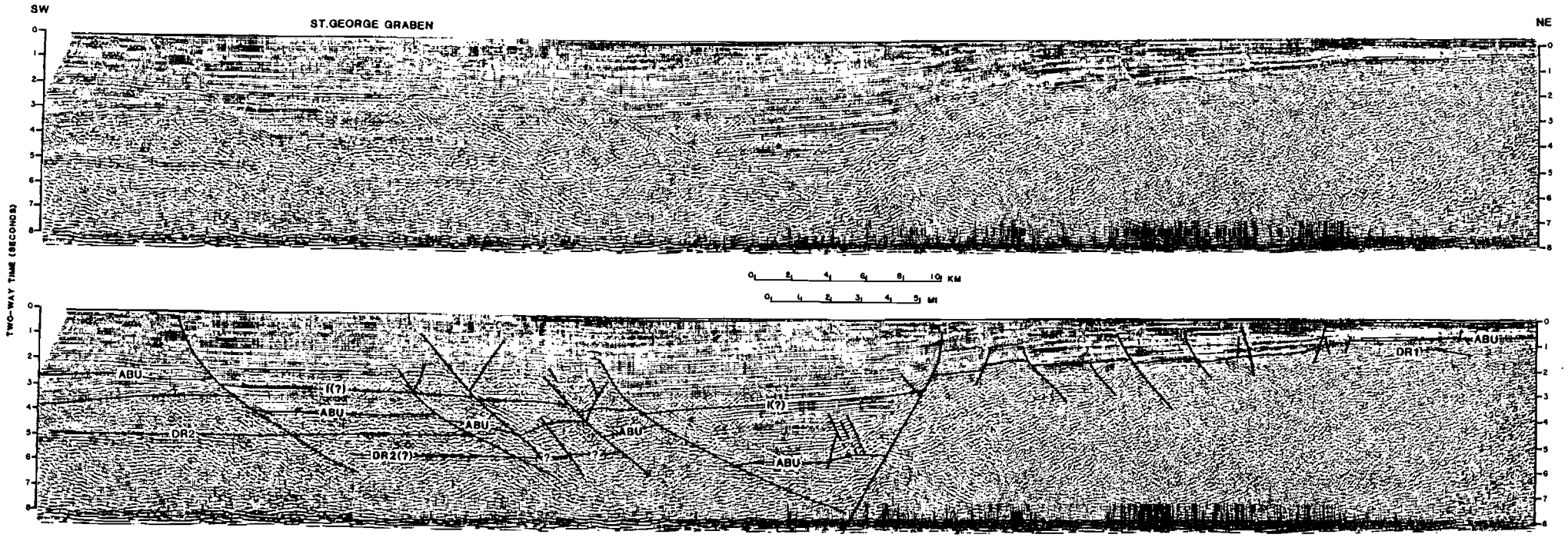

Figure 11. D-D': Migrated seismic profile (courtesy of Western Geophysical Company) illustrating asymmetry of the St. George graben. Note absence of rotation of the southernmost and northernmost fault blocks within the graben. DR1 is thought to be a reflection from the top of an igneous intrusion (?) which is associated with a prominent magnetic anomaly (anomaly 1, fig. 16).

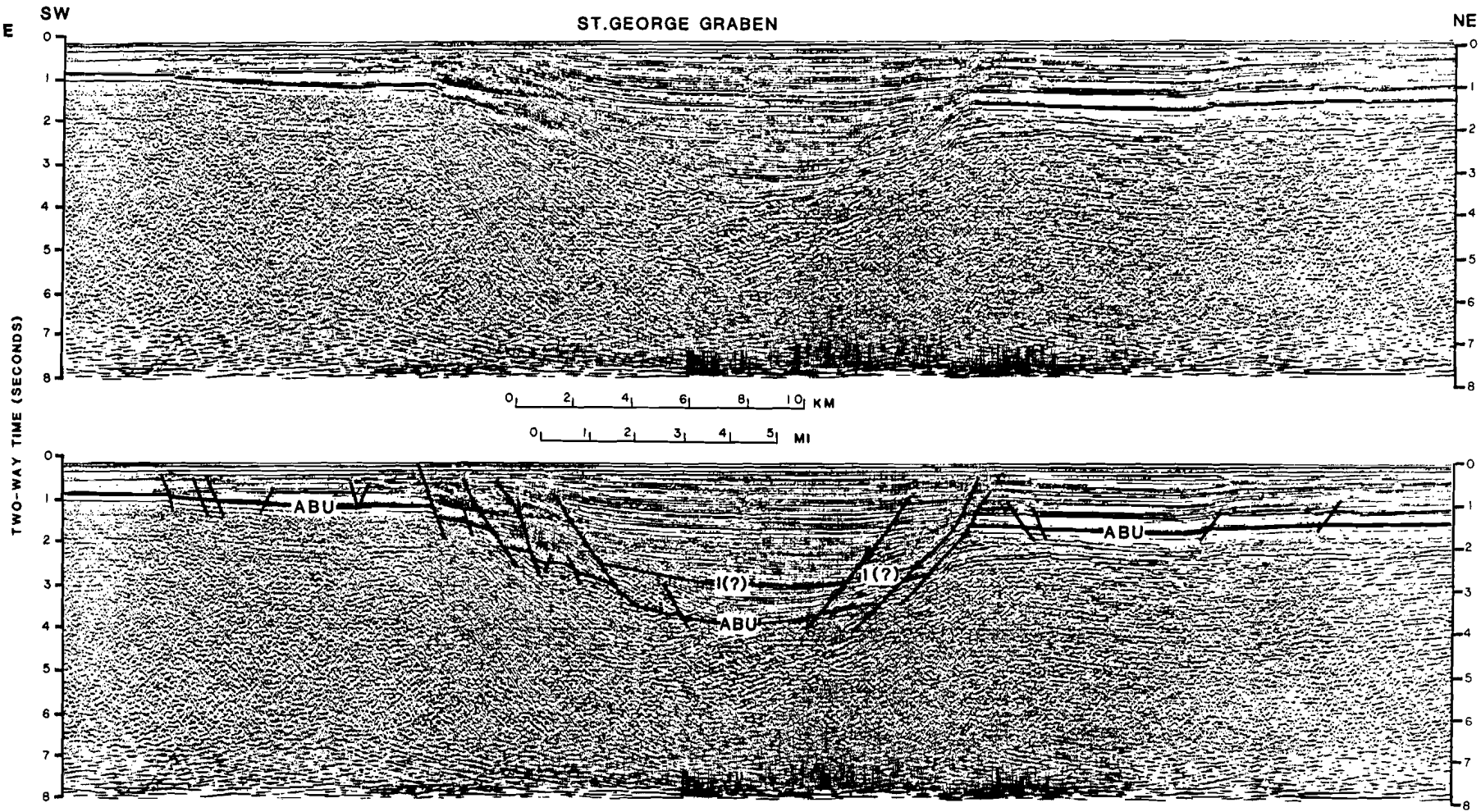

Figure 12. E-E': Migrated seismic profile (courtesy of Western Geophysical Company) illustrating a nearly symmetric profile of the St. George graben, which is common in the northwestern extension of the graben. Note stratal drag along fault planes and absence of rotation of fault blocks.

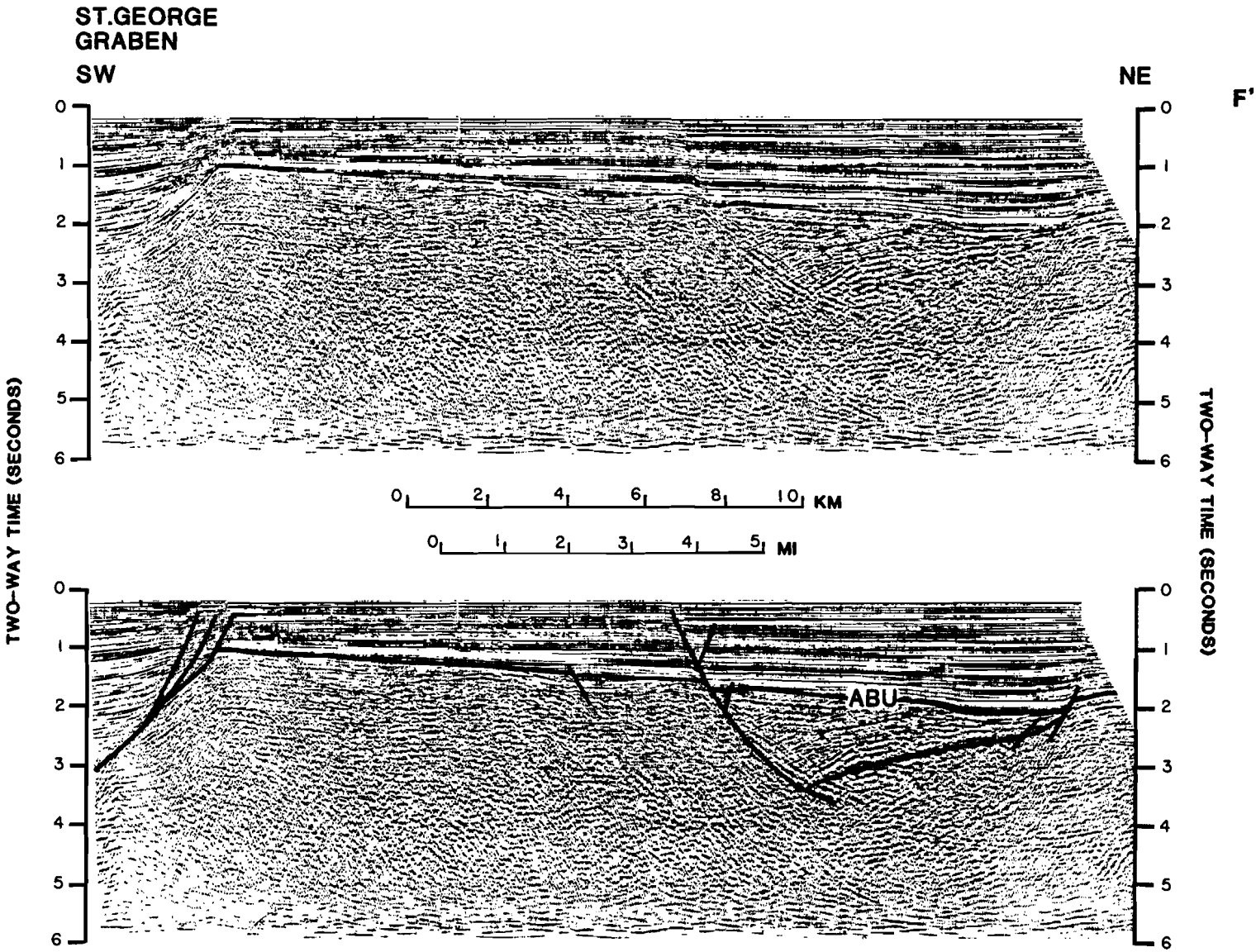

Figure 15. F-F': Migrated seismic profile (courtesy of Western Geophysical Company) illustrating a half-graben below the ABU north of the St. George graben. Interval velocities from strata within the half-graben average 12,500 feet/second, suggesting a Tertiary age. Note the onlap of overlying upper Tertiary strata onto the ABU.

ACOUSTIC BASEMENT

The rocks that make up the acoustic basement underlying the St. George Basin Planning Area are structurally complex. For this reason it is difficult to extrapolate information from the COST wells to determine the age, lithology, and structural relationship of these rocks on a regional scale. The following discussion is based upon several sources of information. In some areas where there are strong seismic reflections below the acoustic basement unconformity, it is possible to determine the interval velocities of the basement rocks. These velocities, along with available seismic data and residual magnetic field data over the St. George basin, indicate the extent of the igneous rocks underlying the planning area. Although preliminary, the interval velocity study also indicates that the acoustic basement unconformity may be younger than previously thought. It has been generally accepted that the acoustic basement consists of rocks of Mesozoic age (Scholl and others, 1975; Marlow and Cooper, 1980), but interval velocities indicate that some of these rocks may be Tertiary. The extent of these younger rocks within the basement is uncertain, because of the preliminary nature of this study and the limited areas where interval velocities can be determined within acoustic basement.

Interpretation of interval velocities from the seismic data used in the following discussion depends to a large part on interval velocities determined at the COST No. 1, COST No. 2, and Exxon Y-0527 and Y-0530 wells (fig. 13). Within the Tertiary section of these wells, velocities range from 7000 to 13,500 feet/second. These velocities lie within a narrow range which increases with depth, indicating that the velocities of these Tertiary units are controlled by compaction and therefore depth of burial. Mesozoic sedimentary rocks have interval velocities which range from approximately 14,000 to 17,500 feet/second. These values are higher for their depth of burial than would be expected from the continuation of the trend of Tertiary velocities, and are much more variable than interval velocities of rocks within the Tertiary section. The interval velocities of volcanic rocks are also higher than those for Tertiary sedimentary rocks. The volcanics at the COST No. 1 well have an interval velocity of 14,700 feet/second, and the volcanics from the Exxon Y-0527 well have an interval velocity of 13,800 feet/second. Thus, seismic stratigraphic units with interval velocities less than 13,500 feet/second are likely to represent Tertiary strata. Rocks with interval velocities greater than this are either volcanics or Mesozoic sedimentary rocks, which can only be distinguished from one another with the magnetic data.

Although the acoustic basement within the St. George Basin Planning Area is characterized by weak, incoherent reflections and multiples, areas exist where structures underlying the acoustic basement unconformity can be recognized on the seismic records. In some areas these reflections are flat-lying (fig. 11). For the most part, however, strong, coherent reflections within the acoustic basement occur as packages of dipping reflections which form an angular unconformity with the relatively flat-lying strata above.

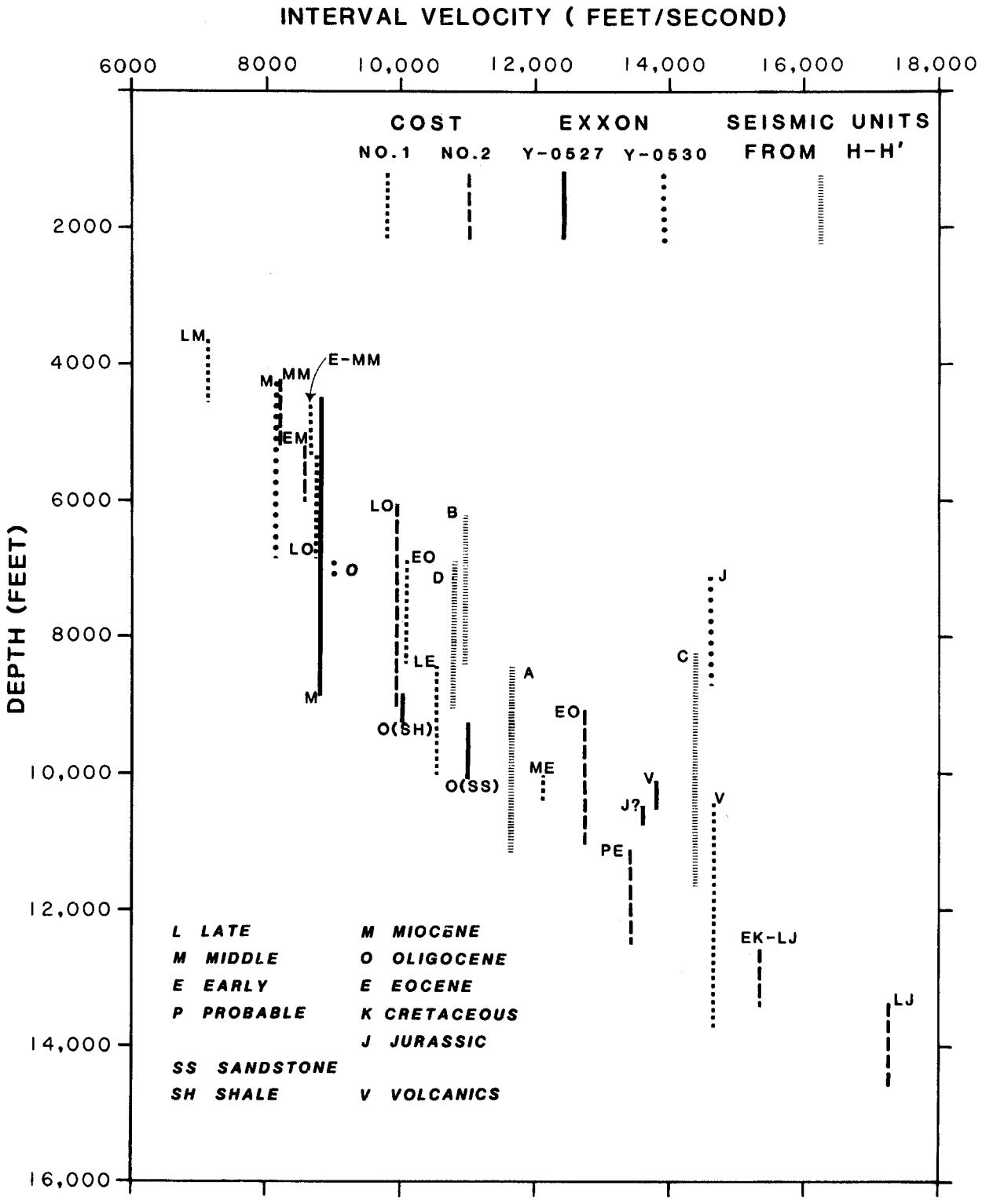

Figure 13. Plot of interval velocities versus depth. COST well and Exxon well velocities are from check shot or vertical seismic profile data. Velocities for seismic units A through D were determined from Western Geophysical Company Velans on and near profile H-H' (fig. 18). Interval velocities are less than 13,500 feet/second for Tertiary sedimentary rocks and greater than 13,500 feet/second for igneous rocks and Mesozoic sedimentary rocks.

Figure 14 shows the outlines of areas north and south of the St. George graben where dipping reflections within the acoustic basement are cut by the acoustic basement unconformity.

North of the St. George graben the packages of dipping reflections are small, and the relationships between them cannot be determined, partly because of faulting. In some cases the reflections die out rapidly with depth; in other areas their dip flattens until they become parallel to the overlying Tertiary section, making them difficult to distinguish from multiples. Some of these packages of dipping reflections are cut by faults and form small half-grabens, such as the one at the north end of figure 15. Interval velocities of the strata within 1 second of the acoustic basement unconformity were calculated at three locations within this half-graben. These values average 12,800 feet/second (s=1000)*, indicating that although they lie below the acoustic basement unconformity, they may be Tertiary strata. How extensive these relatively low velocity rocks are within the acoustic basement is unknown.

A map of the residual magnetic field over the area (Childs and others, 1981) is shown in figure 16. The area north of the St. George graben has a distinct magnetic character of predominantly short-wavelength, high-amplitude anomalies. The maximum amplitude is approximately 1800 gammas (peak to trough), although values between 500 and 1000 gammas are more common. Wavelengths are typically about 20 miles (approximately 30 km). These magnetic anomalies are generally thought to correspond to a Jurassic magmatic arc (Reed and Lanphere, 1973; Marlow and others, 1976) and may also include magmatic arc rocks of Late Cretaceous to Paleogene age (Cooper and others, in press). Alternatively, McLean (1979) argues that although the anomalies may be related to plutonism, the plutonism may not be related to subduction beneath the Beringian margin.

The relationship between these magnetic anomalies and structures visible in the seismic reflection data is unclear. Several of the major anomalies, such as anomaly 1 in figure 16, occur over slightly domed reflections apparent on the seismic data (horizon DR1 at the NE end of figure 11). The antiformal reflections may represent strata domed as a result of igneous intrusion, or may correspond to the top of the igneous body itself. The overall lack of coherent reflections which characterizes the acoustic basement north of the graben may be caused by the presence of igneous rocks. However, it is also possible that a strongly reflective acoustic basement unconformity prevents the penetration of acoustic energy into the basement.

The pattern of high-amplitude, short-wavelength magnetic anomalies changes abruptly toward the southwest, which gives the appearance that the magmatic rocks may have been faulted along their southern margin. The northern boundary fault of the St. George graben lies near the -200-gamma contour, however, 5 to 10 miles south

*s=twice the standard deviation for certainty within the 95th percentile.

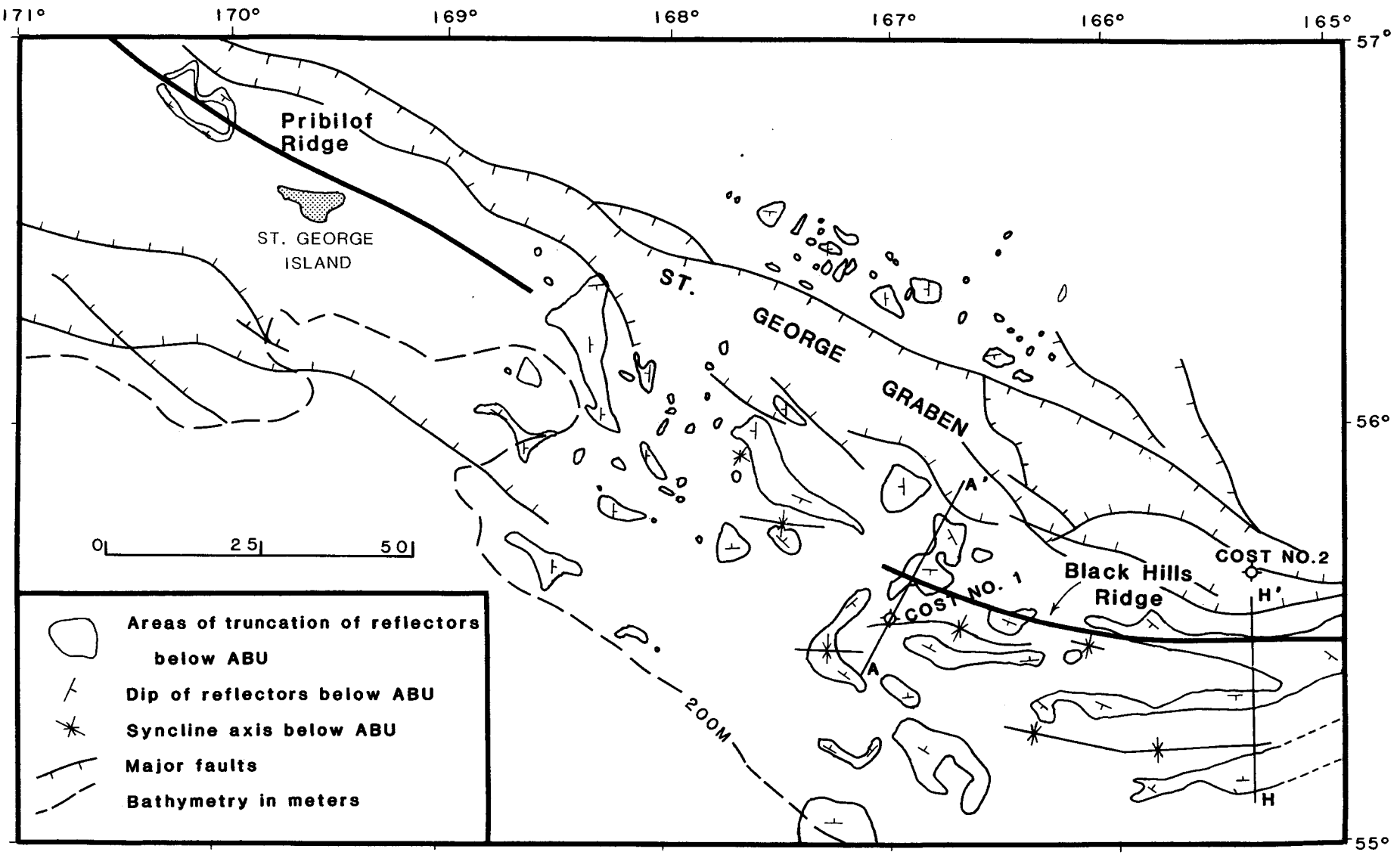

Figure 14. Map showing outlines of areas where the ABU truncates dipping reflections. Velocity analyses suggest that some of the reflections below the ABU may be from lower Tertiary strata. Magnetic anomaly data indicate that igneous rocks are locally significant (fig. 16). The Black Hills ridge is not an anticlinal structure; reflections from within the ridge dip to the south.

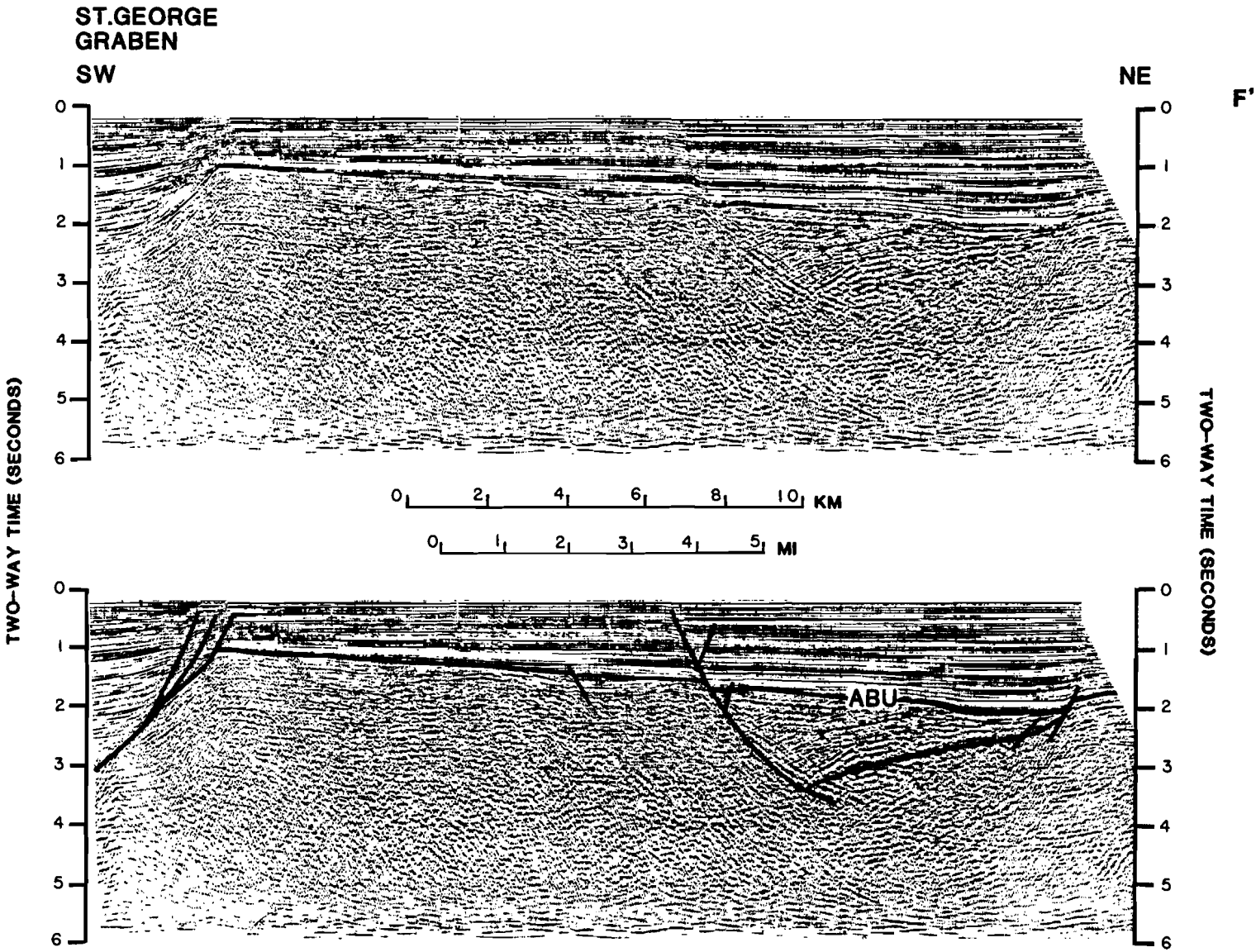

Figure 15. F-F': Migrated seismic profile (courtesy of Western Geophysical Company) illustrating a half-graben below the ABU north of the St. George graben. Interval velocities from strata within the half-graben average 12,500 feet/second, suggesting a Tertiary age. Note the onlap of overlying upper Tertiary strata onto the ABU.

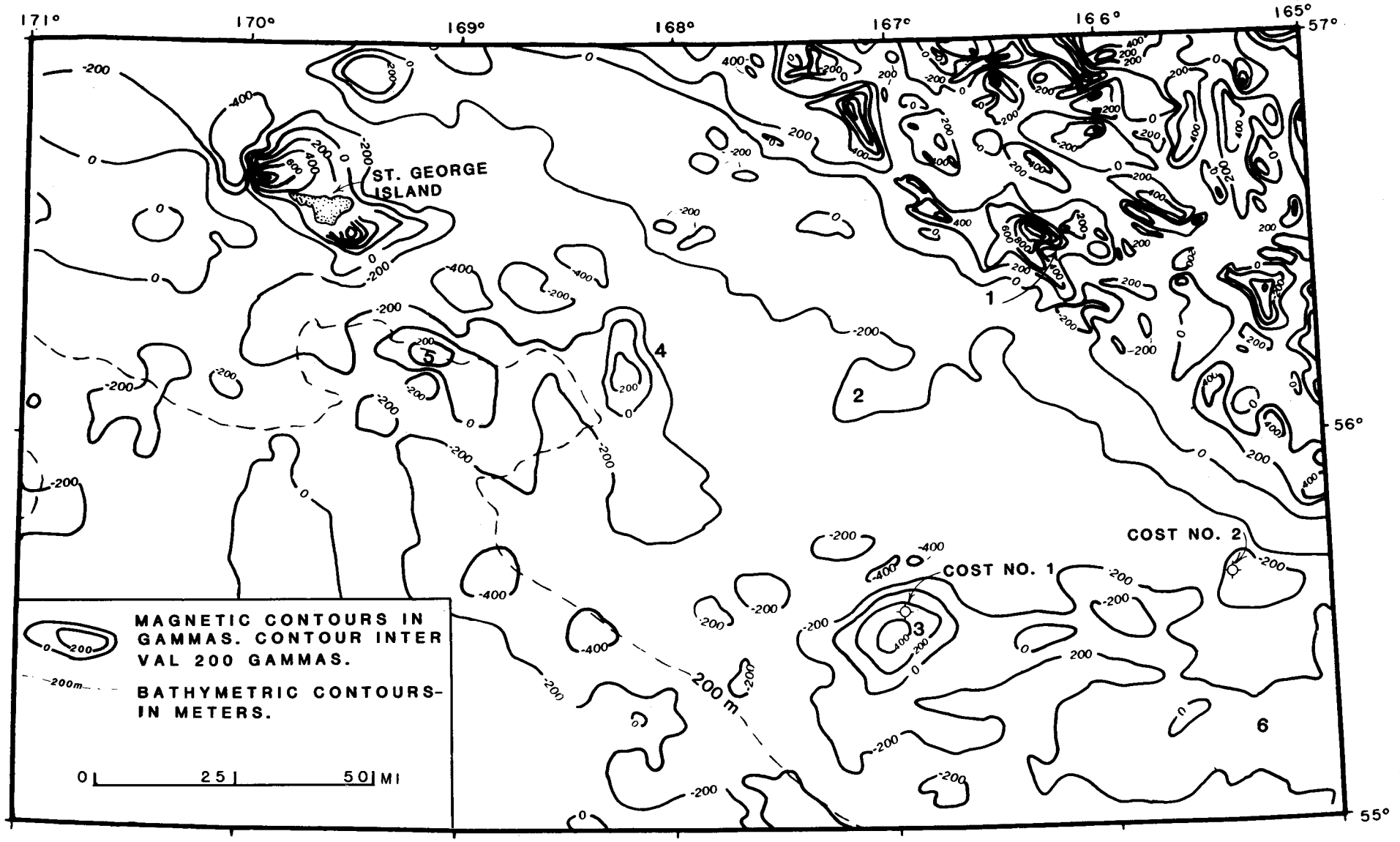

Figure 16. Residual magnetic field map of the St. George basin (adapted from Childs and others, 1981). Anomaly 1 is over a possible igneous intrusion (fig. 11). Anomaly 2 is over a possible sequence of igneous flows or sills (fig. 17). Anomaly 3 is over an eroded volcanic edifice at the COST No. 1 well (fig. 7a). Anomalies 4 and 5 are other possible volcanic edifices. Anomaly 6 is over a synformal structure below the ABU south of the Black Hills ridge (fig. 18). Interval velocities on profile H-H' (fig. 18) immediately below the ABU average 14,700 feet/second, which is consistent with igneous rocks of the COST No. 1 well (fig. 13).

of this change in anomaly pattern. Thus it appears that this change in magnetic character is not structurally related to the graben itself.

Anomaly 2 in figure 16 is a relatively low-amplitude feature that projects into the St. George graben. Figure 17 shows a seismic profile that crosses the anomaly from southwest to northeast. The northern boundary fault of the graben is indicated by the heavy fault line in the figure. North of this fault the regional unconformity dips toward the south, and is cut by the fault at 2.3 seconds (two-way travel time). South of the fault no coherent reflections are seen below 1.2 to 1.5 seconds, which is shallower than the regional unconformity on the upthrown side of the fault. The coincidence of the magnetic anomaly and shallow, strong reflections suggests that these reflections may be caused by basalts or other highly magnetic igneous rocks interlayered with the sediments filling the graben. If so, it is unclear from the available data whether these rocks are flows or sills.

South of the graben, areas where the acoustic basement unconformity truncates underlying reflections are larger than to the north (fig. 14). Although many occur as isolated packages, as they do north of the graben, in some cases the reflections below the unconformity can be followed for long distances, and some appear to define broad west- to northwest-trending folds. This area is characterized by lower amplitude, longer wavelength magnetic anomalies than the area north of the graben. Anomaly amplitudes are 300 to 500 gammas with several local anomalies as great as 700 gammas. Wavelengths are 50 to 70 miles (approximately 100 km).

Antiforms below acoustic basement are difficult to identify. Their presence is suggested by reflective packages dipping away from one another, but reflections between them do not have adequate coherence to be traced from one limb to the next. The reflective strata may have been eroded away at the crests of anticlinal folds, or the packages may not be correlatable because of intervening faults. Synforms are more easily identified. In some areas reflections are continuous between two inwardly dipping packages. In other areas only the shallowest reflections are continuous, the deeper reflections losing coherency with depth. Other synforms appear to be cut by faults but retain the synformal structure (figure 18). There are also many areas where synforms are suggested by inwardly dipping packages of reflections that are completely separated by incoherent noise.

The axes of clearly identifiable synforms are shown in figure 14. The COST No. 1 well was drilled into one of these, as shown on seismic profile A-A' (fig. 7a). A comparison of figures 14 and 16 shows that anomaly 3, which is circular in plan view, encompasses the site of the COST No. 1 well. The crest of the magnetic anomaly occurs over the southern edge of the synform into which the COST No. 1 well was drilled. The well encountered basalts and pyroclastics from 10,380 feet, which is just below the regional unconformity, to total depth (13,771 feet).

Interval velocities within the basalt determined from the sonic log range from 13,000 to 16,000 feet/second (Comer, 1984b). The interval velocity determined from the check shot survey over the depth range in which basalts were encountered is 14,700 feet/second. Figure 7a shows that reflections from within the basalts appear to continue to the northern flank of the synform, where they are truncated by the acoustic basement unconformity. To the south these reflections continue past the southern edge of the synform, where they become approximately parallel to the acoustic basement unconformity. Interval velocity values in this unit of rocks were calculated from seismic velocity spectra displays at 9 points along and to the south of the synform. Each interval extended approximately 0.5 second below the acoustic basement unconformity. The average interval velocity for the unit is 15,000 feet/second (s=1300 feet/second), which is consistent with velocities for the basalt penetrated by the COST No. 1 well.

The basalts at the COST No. 1 well are laterally continuous with a well-stratified section to the north that is also below the regional unconformity (fig. 7a). The interval velocity of this northern package is about 12,500 feet/second, which is similar to that of Eocene rocks in both the COST wells. As velocities of basalts and Mesozoic sedimentary rocks are greater than 13,500 feet/second, the relatively low-velocity rocks beneath the unconformity are likely to be early Tertiary. Because these rocks appear stratigraphically equivalent with the COST No. 1 well basalts, the basalts are likely to be early Tertiary also.

The presence of volcanics within and to the south of the synform indicates that the magnetic anomaly is related to a buried, eroded volcanic edifice. Acoustic layering within the volcanics is probably related to impedance contrasts across boundaries between massive basalts and brecciated basalts or pyroclastic layers. St. George Island, where Cox and others (1966) found Pliocene basalts, is also associated with a major magnetic anomaly (fig. 16). Anomalies 4 and 5 are circular, positive anomalies similar to anomaly 3, and may also be old volcanic centers.

The longest of the synforms shown in figure 14 is located just south of the Black Hills ridge and can be traced for approximately 30 miles. Seismic line H-H' (fig. 18) crosses it and shows that it is a broad feature defined by reflections that are, for the most part, continuous and that extend to depths in excess of 5.0 seconds (approximately 30,000 feet). Elsewhere along the strike of the synform, the strata are more complexly deformed. Interval velocities of rocks within the synform are highly variable and difficult to interpret. In figure 18, seismic unit A lies between unconformity II(?) and the acoustic basement unconformity. Velocity spectra displays were interpreted for 8 points along the section shown in figure 18 and adjacent seismic sections. The average interval velocity for unit A is 11,700 feet/second (s=2300 feet/second). This interval velocity is similar to the interval velocity of the rocks just above basement in the COST No. 1 well (fig. 13), and is well within the range of velocities expected at that depth for Tertiary

sedimentary rocks. Coherent reflections below the acoustic basement unconformity extend to considerable depths, but velocity data are difficult to interpret more than 0.5 second below the unconformity. The average of seven interval velocities measured within this 0.5-second unit is 14,700 feet/second (s=2300 feet/second), which is consistent with either Mesozoic sedimentary rocks or volcanic rocks. The synform generally coincides with broad, east-west-trending magnetic anomaly 6 (fig. 16). This correlation with a positive anomaly indicates that the rocks underlying the acoustic basement unconformity are probably volcanic.

The Black Hills ridge consists of southwardly dipping beds which are truncated on the north flank of the ridge by the northwardly dipping acoustic basement unconformity (figs. 7a and 18). A comparison of figures 14 and 16 shows that the ridge is approximately coincident with a magnetic trough, indicating that these rocks are different from those which form the synform to the south. It was possible to calculate the interval velocity of rocks underlying the Black Hills ridge within three seismic units, labeled B, C, and D in figure 18. The average of five interval velocities from unit B at the crest of the Black Hills ridge is 10,900 feet/second (s=3000 feet/second). Below unit B, the interval velocities in unit C are higher, averaging 14,400 feet/second (s=1600 feet/second). Interval velocities north of the crest of the Black Hills ridge are difficult to determine because of faulting, but the average of five interval velocities near the northern end of figure 18 (unit D) is 10,800 feet/second (s=2200 feet/second). The interval velocities for these units and for unit A have been plotted on figure 13, using the average depth calculated for the top and bottom of each interval. Units A, B, and D plot well within the narrow range of Tertiary interval velocities from the wells. This result was expected for unit A, which lies above the acoustic basement unconformity, but not for units B and D. Although they are part of the acoustic basement, the interval velocities of these rocks indicate that they may be Tertiary in age. How extensive these Tertiary rocks are within the basement is unknown because of the preliminary nature of this study. The velocity for unit C falls above the Tertiary velocity/depth curve. Although both volcanics and Mesozoic sedimentary rocks lie in this range, its location in a magnetic trough is interpreted to mean that unit C is composed of Mesozoic sedimentary rocks.

All of the reflections discussed above generally lie within a few seconds of the acoustic basement unconformity. Throughout most of the planning area these reflections are the deepest features apparent on the seismic data. However, in two areas south of the St. George graben, a series of continuous reflections occurs at roughly 5.0 seconds. Velocity analyses, as well as their shallow dip in comparison to the overlying reflections, indicate that these are not multiples. One set of deep reflections occurs between 166° and 168° W longitude. These deep reflections, shown in figure 7a (DR2), end abruptly about 15 miles south of the graben. In other areas they die out gradually to the south, but never extend far from the graben. Throughout much of the area they are at a depth of about 30,000 feet, but they become more shallow to the west, where they approach 4.0

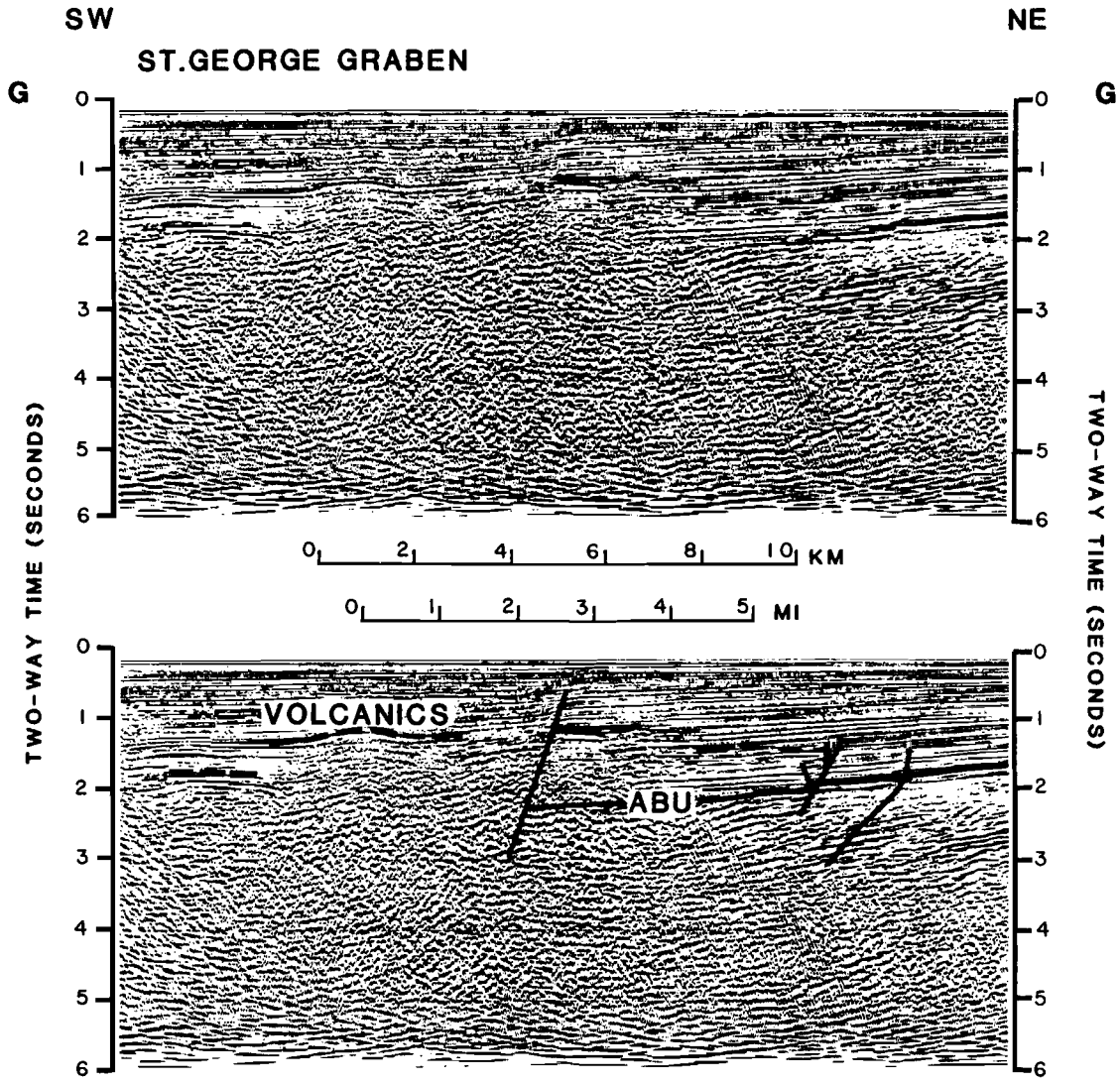

Figure 17. G-G': Migrated seismic profile (courtesy of Western Geophysical Company) showing shallow strong reflections, interpreted to be igneous flows or sills, that correspond to magnetic anomaly 2 in figure 16.

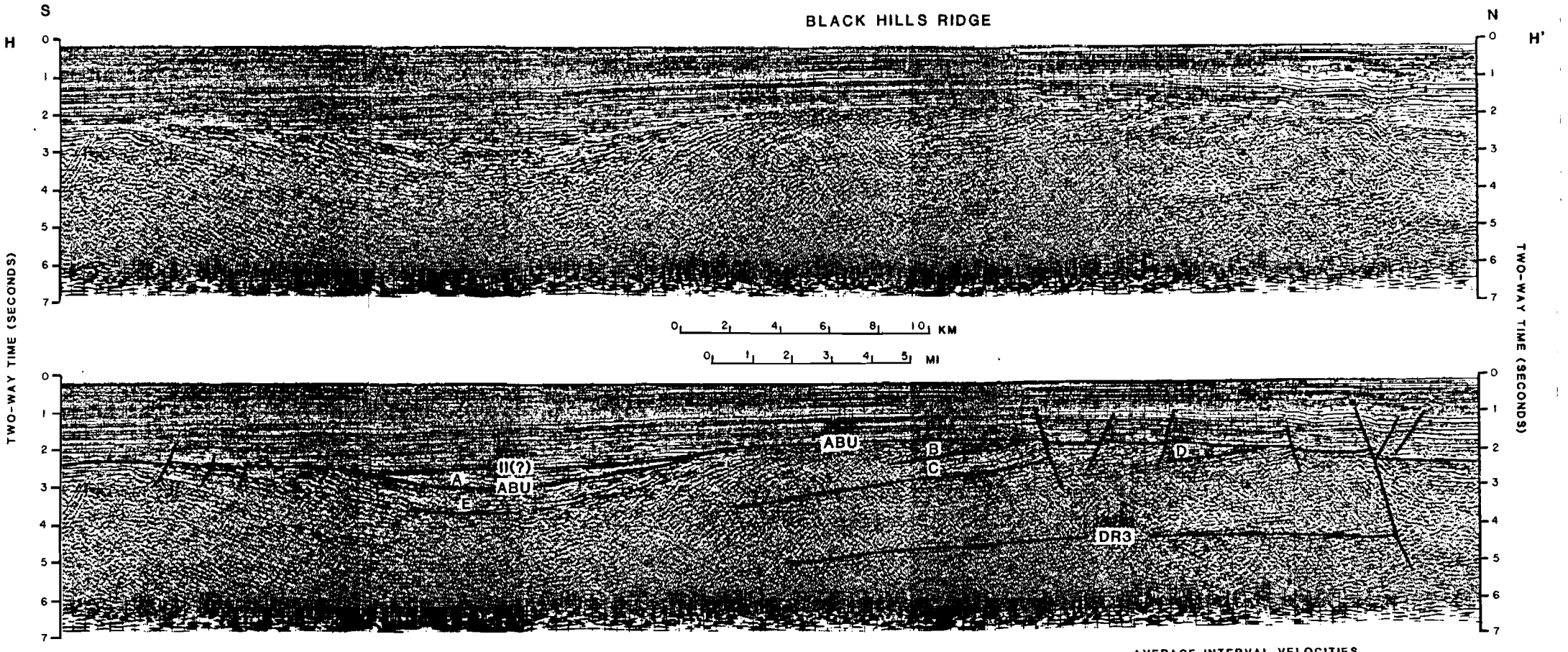

Figure 18. Migrated seismic profile (courtesy of Western Geophysical Company) showing seismic stratigraphic units below the ABU (units B and D) that have interval velocities consistent with Tertiary strata (fig. 13). Unit A, above the ABU, has an average velocity consistent with middle and late Eocene strata of the COST No. 1 well (figs. 7a and 13). Units C and E have velocities consistent with either igneous rocks or Mesozoic sedimentary rocks. The absence of a magnetic anomaly over unit C implies Mesozoic sedimentary rocks; the presence of a magnetic anomaly (anomaly 6, fig. 16) over unit E implies igneous rocks.

AVERAGE INTERVAL VELOCITIES

UNIT	VELOCITY (FEET/SECOND)
A	11,700
B	10,900
C	14,400
D	10,800
E	14,700

seconds (23,000 feet). There are similar deep reflections to the east, between 165° and 166° W longitude, shown in figure 18 (DR3), but available seismic data do not allow correlation of the deep reflections from one area to the next. In the western area, the deep reflections are overlain by a thick, acoustically transparent sequence with interval velocities ranging from 17,000 to 18,000 feet/second. In the eastern area, velocity data are very difficult to interpret at this depth, but it appears that the interval velocities above this deepest reflection are slower, averaging approximately 15,000 feet/second. The cause of these deep reflections cannot be determined with any certainty. Page and others (1986) use refraction seismic data from the northern Chugach Mountains and southern Copper River basin to identify horizontal low-velocity zones below the Chugach and Peninsular/Wrangellia terranes. They interpret the shallowest of these zones, which is at a depth similar to the deep reflections discussed above, as a possible decollement zone. It is highly speculative, but plausible, that the deep reflections in the basement rocks underlying the St. George basin are from a similar decollement zone beneath the Peninsular terrane.

GEOLOGIC HISTORY

Basement rocks in the St. George Basin Planning Area include rocks equivalent to the Late Jurassic Naknek Formation, the Late Jurassic and Early Cretaceous Staniukovich Formation, and the Late Cretaceous Hoodoo Formation. These formations and the Lower and Middle Jurassic igneous rocks on the Alaska Peninsula compose the Peninsular terrane as defined by Jones and Silberling (1979). Wilson and others (1985) partially redefined the terrane and proposed that it be called the Alaska Peninsula terrane. Paleomagnetic pole locations determined from Peninsular terrane rocks indicate that the terrane originated in the southern hemisphere (Packer, 1972; Packer and Stone, 1974; Stone and Packer, 1977, 1979; Stone and others, 1982). From there, the Peninsular terrane migrated northward relative to the North American craton beginning in the Late Jurassic. Prior to its collision with the craton, the terrane collided and subsequently coalesced with the Prince William-Chugach and the Wrangellia terranes. This superterrane is believed to have finally collided with the North American craton roughly 60 m.y.b.p. (Hillhouse and Coe, in press).

The St. George graben and the Pribilof basin are thought to have opened during a period of strike-slip or oblique-slip motion between the Kula plate and North America, which occurred along the Beringian margin (Marlow and Cooper, 1980). However, age estimates for the timing of the opening vary considerably. Marlow and Cooper (1980) proposed that strike-slip motion and the initial graben formation began in the late Mesozoic to early Tertiary. Strike-slip motion subsequently ceased as the Kula plate became locked along the Beringian margin as a result of the formation of the Aleutian Island arc. Marlow and Cooper (1983) believe the initial formation of the arc began at least by earliest Tertiary time. Alternatively, Whitney

and Wallace (1984) date events by correlating the change in strike of the Hawaiian-Emperor seamount chain with a change in motion of the Pacific plate relative to the hot-spot reference frame. This change in plate motion occurred at 43 m.y.b.p., and would have produced a change from oblique subduction to strike slip along the Beringian margin. During the time of oblique subduction (56 to 43 m.y.b.p.), there was no volcanism in either the Kuskokwim Mountains or the Alaska Range. The St. George graben opened during the subsequent period of strike-slip motion, which lasted from 43 to 42 m.y.b.p. It is at this time that Whitney and Wallace (1984) propose that the Aleutian arc formed. Yet another interpretation is given by Harbert and others (1985), who used the relative rotations between the North American plate and the Eurasian plate in order to estimate the relative motion between the North American plate and the Kula plate. Their results indicate that the period of strike-slip motion occurred between 50 and 37 m.y.b.p.

The time of opening of the St. George graben can be constrained by geologic data if it is assumed that the regional unconformity at the top of acoustic basement resulted from uplift associated with rifting. The initial stage of continental rifting is often accompanied by regional uplift: examples include the formation of the East African Rift (Brown and Girdler, 1980; Mohr, 1982) and the Red Sea (Cochran, 1983). These rifts, however, differ from the St. George graben in that they opened because of regional extensional forces, whereas the St. George graben opened in a strike-slip fault system in which extension was local rather than regional. It is not certain, therefore, that the regional unconformity is directly related to the opening of the graben. Given that caveat, we interpret the occurrence of middle Eocene sedimentary rocks above the unconformity at the COST No. 1 well and early Eocene sedimentary rocks above the unconformity at the COST No. 2 well to indicate that the graben opened before the end of the early Eocene. The earlier age within the graben at the COST No. 2 well is consistent with the graben being a depositional site before the area outside the graben, such as at the COST No. 1 well. The earliest that the graben opened may be Paleocene, based on possible Paleocene rocks below the unconformity at the COST No. 2 well (J. Bujak, written commun., 1986). This interpretation is consistent with the timing proposed by Marlow and Cooper (1980), but differs from that proposed by Whitney and Wallace (1984) and Harbert and others (1985).

The initial subsidence in the graben was probably fairly rapid, based on the greater amount of offset on the deeper segments of the faults and the seismic-reflection character of the deep strata in the graben. Low-frequency reflections from Oligocene and older strata (for example, horizon I in fig. 7b and fig. 11) are interpreted to be massively bedded, coarse clastics shed from the topographically high north wall of the graben. Above these strata, the higher frequency reflection character indicates deposition of finer grained marine strata, which can be traced outside the graben to the COST No. 1 well (fig. 7a). We believe that subsidence in the graben slowed considerably by the late Oligocene, which is the age of horizon I at the COST No. 1 well. The area in which the graben first opened is

presently the deepest portion of the graben (fig. 10). Following the period of strike-slip motion, simple extension continued in the graben, as evidenced by normal faults that extend to the sea floor.

The cross section of the Pribilof basin (fig. 9) is very similar to that of the continental borderland basins of southern California, which developed on a transform margin (Howell and others, 1980). By analogy, we believe that the Pribilof basin opened in response to strike-slip motion along the Beringian margin. It has not been possible to correlate the deeper reflective horizons of the Pribilof basin with the COST wells, so the time of its opening is not as well constrained as that of the St. George graben.

2. Petroleum Geology

The assessment of reservoir rock potential and source rock quality and maturation in the St. George Basin Planning Area is based primarily on data from the St. George basin COST wells. The COST No. 1 well was drilled about 20 miles south of the graben and penetrated about 10,000 feet of volcaniclastic Cenozoic sediment overlying basaltic basement rock. The COST No. 2 well was drilled within the first set of faults on the south flank of the graben, and penetrated more than 12,000 feet of volcaniclastic Cenozoic sediment and more than 2000 feet of the underlying Mesozoic sedimentary rocks. Additional information has recently been released from two Exxon wells in the graben, and it is summarized in the Exxon Wells section of this report. The discussion of trap types is based on our interpretation of seismic reflection data; these data have been correlated to the COST well stratigraphy to evaluate the timing of potential hydrocarbon generation and migration relative to trap development.

RESERVOIR ROCK POTENTIAL

The assessment of the reservoir rock potential at the COST wells is based on the detection of porous and permeable sandstones on the spontaneous potential (SP) log or in cores and cuttings from the wells. Direct measurements of porosity were made from sidewall and conventional cores, and measurements of permeability were made from conventional cores. We do not consider the permeability measurements from the sidewall cores to be reliable. The log data, collected by Schlumberger, and the porosity and permeability measurements (Core Laboratories, 1976; AGAT, 1982) were reviewed by Bolm (1984a, 1984b). These form the basis for our discussion of the reservoir rock potential in the vicinity of the two wells. Unless noted otherwise, extrapolations away from the wells are our own and are based on an analysis of the character of seismic reflections.

The porosity of sedimentary rocks generally decreases with increasing depth. The primary cause for porosity loss is compaction, partly a result of deformation of ductile grains caused by the weight of the overburden. Sediments on the Bering shelf within the St. George Basin Planning Area are mostly volcaniclastic siltstones and silty sandstones with high ductile-grain content. Table 1 shows average porosity and permeability values for the various

TABLE 1. Porosity, permeability, and gross sand, St. George Basin COST No. 1 and No. 2 wells.

Epoch	COST Well	Sample Type[1]	Depth Interval[2] (ft.)	No. of Samples	Thickness (ft.)	Porosity[3] (%)	Permeability[3] (mD)	Gross Sand[4] (ft.)	Gross Sand (%)	Range of Bed Thicknesses[5] (ft.)	
Pliocene	1	SW	1,600-3,600	15	2,000	37.9 ± 2.7	23 ± 17	1,125	56	5-10	
	2	SW	1,460-4,246	13	2,786	37.3 ± 3.0	81 ± 82	1,525	55	10-50	
	2	C	4,104-4,129	26	---	37.7 ± 2.0	7 ± 6	---	--	---	
Miocene	1	SW	3,600-5,370	21	1,770	34.1 ± 5.0	36 ± 31	775	44	5-90	Most beds <30 ft. thick.
	1	C	4,105-4,134	14	---	37.0 ± 1.5	78 ± 55	---	--	---	
	2	SW	4,246-6,050	7	1,804	27.8 ± 2.1	96 ± 21	200	11	5-15	Most beds found between 4,840 ft. and 5,465 ft.
	2	C	5,155-5,184	9	---	28.6 ± 1.8	30 ± 34	---	--	---	
Oligocene	1	SW	5,370-8,410	62	3,040	27.9 ± 4.1	158 ± 221[6]	1,650	54	5-350	1,200 ft. of gross sand in beds thicker than 150 ft.
	1	C	5,669-7,919	176	---	24.8 ± 6.4	31 ± 69[7]	---	--	---	
	2	SW	6,050-11,085	43	5,035	24.9 ± 2.7	42 ± 29	1,630	32	5-120	Most abundant at depths >7,850 ft.
	2	C	6,650-10,627	116	---	17.5 ± 5.2	2 ± 6	---	--	---	
Oligocene or older (Eocene?)	2	SW	11,085-12,540	11	1,455	21.8 ± 2.3	62 ± 32[8]	220	15	10-60	
	2	C	11,702-12,448	54	---	13.1 ± 0.8	2 ± 2	---	--	---	
Eocene	1	SW	8,410-10,380	15	1,970	23.9 ± 2.2	18 ± 20	450	23	5-100	
	1	C	9,646-10,375	61	---	16.7 ± 3.7	2 ± 11	---	--	---	

Early Cretaceous to Late Jurassic	2	SW	12,540-13,370	4	830	22.8 ± 2.3	54 ± 35[9]	250	30	40-100	Logs indicate no porosity.
	2	C	12,571-12,594	9	---	7.7 ± 2.2	1 ± 1	---	--	---	
Late Jurassic	2	SW	13,370-14,626	8	1,256	21.4 ± 4.0	121 ± 74[10]	---	--	---	
	2	C	13,559-14,619	31	---	5.4 ± 2.5	1 ± 1	---	--	---	

1. SW = sidewall core; C= conventional core.

2. For conventional cores, the depth interval corresponds to the depth range of the samples. For sidewall cores, the depth interval corresponds to the total depth range for any given age in the well.

3. The mean and one standard deviation are listed.

4. Total thickness of gross sand as detected with SP log.

5. Thicknesses refer to beds of gross sand.

6. Only 61 permeability measurements.

7. Only 175 permeability measurements.

8. Permeability was measured in only 8 samples.

9. Permeability was measured in only 2 samples.

10. Permeability was measured in only 3 samples.

time-stratigraphic units identified in the two St. George COST wells. The rate of porosity loss with increasing depth in the St. George basin is approximately 3 percent/1000 feet. This value is three times greater than the rate of loss determined in the COST No. B2 well on the Atlantic OCS (Rhodehamel, 1977). The greater porosity loss rate in the St. George basin is probably a consequence of the high ductile-grain content and of the growth of secondary minerals, such as zeolites and clays, in the interstitial spaces. Such minerals are produced from the interaction of pore water and volcanic rock fragments. They decrease not only the porosity, but also the permeability.

Table 1 also shows the gross sand thicknesses, the fractional amount of gross sand expressed in percent, and the range of thicknesses of the gross sand beds of each epoch. The table is based on data presented by Bolm (1984a, 1984b). Gross sands were identified primarily on the SP log. Table 1 shows that Miocene and older rocks at the COST No. 1 well have a considerably greater percentage of gross sand than coeval rocks from the COST No. 2 well. At the COST No. 1 well, the Oligocene section has the best reservoir characteristics. Approximately 1250 feet of the gross sands are in beds thicker than 150 feet. Samples recovered from conventional cores have favorable porosities, averaging 25 percent, and permeabilities, averaging 31 millidarcies (mD). Oligocene rocks in the COST No. 2 well have comparable sand thicknesses. However, the average porosity and permeability measured from conventional cores, 17 percent and 2 mD respectively, are significantly lower in the COST No. 2 well. The reasons for the apparently poorer reservoir quality of the Oligocene section at the COST No. 2 well are not presently known. It may be that the deeper burial of sediment at the COST No. 2 site, approximately 2000 feet for the Oligocene section, resulted in more adverse diagenetic alterations than in sediment at the COST No. 1 site. Indeed, it appears from the core data that at the COST No. 2 well the Miocene section has better reservoir potential than the Oligocene section (table 1).

Reservoir rock data from the two Exxon wells are more limited than for the COST wells because fewer conventional cores were taken. The first well (Y-0530) cored a basal Tertiary conglomerate which had an average porosity of 7.5 percent and a permeability of less than 1 mD. This well also cored a Jurassic siltstone which had an average porosity of about 5 percent and essentially no permeability. There were no permeable sands apparent on the SP log in the Tertiary section. The second well (Y-0527) cored a Miocene sandy siltstone which had porosities ranging from 18 to 22 percent and permeabilities of less than 3 mD. A sandy section in the lower Oligocene is apparent from the SP log. The sand beds range from 5 to 20 feet thick for a gross total of 185 feet. Twenty-three sidewall cores in this sandy zone had an average porosity of about 24 percent.

Conclusions drawn for reservoir quality at the COST wells and the two Exxon wells may not be directly applicable to other areas of the graben. The COST No. 1 well was drilled on a stable but subsiding shelf south of the graben. The COST No. 2 well was drilled

within the first of a series of faults that form the southwestern boundary of the graben. The Exxon wells were drilled in the graben on a structural high that has a relatively thin Tertiary section. Data from these wells are not thought to be representative of the deeper portions of the graben, which generally occur on the downthrown side of the northern boundary fault. Seismic horizons tied to COST well data have been extended into the graben (figs. 7a and 7b). From these dated seismic horizons, it appears that the initial opening and subsidence of the graben occurred rapidly. Low-frequency, high-amplitude reflections from Oligocene and older strata suggest deposition of massively bedded sediment. While part of the low-frequency character of these reflections is due to high-frequency attenuation of the seismic source, we believe that massively bedded, coarse clastics are primarily responsible for this seismic signature. These rocks were probably eroded from lower Tertiary and Mesozoic highs that flanked the graben. If so, they are recycled volcaniclastic detritus. Erosion of sedimentary rocks and subsequent redeposition generally leads to sediment with a higher quartz content and a lower clay content. Reservoir quality of the rocks within the graben would therefore be enhanced relative to the rocks outside the graben. The Exxon wells, although located in the graben, did not encounter the lower Tertiary section that causes the low-frequency seismic signature.

Rapid deposition, which occurred in the graben, may also be a favorable factor for reservoir rock potential. Rapidly deposited sediments are sometimes unable to lose sufficient interstitial water for compaction to proceed at its normal rate. Consequently, the sediments would retain a relatively high porosity and have a correspondingly high capacity for oil and gas. Abnormally high pore pressure is another result of this process, but there is no evidence for abnormally pressured sediments in St. George basin.

Although there are several reasons to suspect that the reservoir potential in parts of the St. George graben may exceed that found at the COST wells, there are no data at present to support this conclusion. Indeed, the porosity and permeability of the rocks causing the low-frequency seismic reflections discussed above could be rather low if the sediments were deposited too near their source to have been well sorted, because poorly sorted sediments typically have low porosities and permeabilities.

In summary, the porosity and particularly the permeability of the volcaniclastic sediments in the planning area have been substantially reduced by the growth of secondary minerals and the deformation of ductile framework grains caused by burial. Oligocene strata in the area of the COST No. 1 well have the best measured porosity and permeability. Near the COST No. 2 well, the overall reservoir potential is best in the Miocene, although it is not as prospective as the Oligocene at the COST No. 1 well. The reservoir potential within most of the St. George graben is unknown. High-amplitude seismic reflections from Oligocene and older strata suggest the presence of massively bedded coarse sediments which may have good reservoir potential.

SOURCE ROCK POTENTIAL

Potential at the COST Wells

The two COST wells provide the only direct evidence on source rock potential for the St. George basin. No geochemical data are available from the Exxon wells. The Cenozoic sediments in both COST wells were deposited in an open-marine, mostly neritic environment. Shelf sediments are rarely good source beds for oil because much of the organic input is from non-aquatic terrestrial plants, and deposition usually occurs under oxidizing conditions. According to Demaison (1981), these two factors favor a gas-prone source rock, which he has termed a "type C" organic facies. Planktonic organic matter, which is oil prone, is biogenically degraded when deposited in an oxygenated shelf environment. The geochemical data from the COST wells indicate that the sediments contain only relatively low amounts of gas-prone organic matter (Banet, 1984; Flett, 1984). The following discussion is a brief review of the geochemical analyses performed on the rock samples recovered from the two COST wells.

Organic Carbon

The total organic carbon (TOC) content for sediment samples from the COST No. 1 well is usually less than 0.5 percent, except for the section from 9000 to 9600 feet, where the highest recorded TOC value is 0.74 percent (Banet, 1984). In the COST No. 2 well, TOC values in Tertiary sediments are generally less than 0.5 percent, except for sections between 5000 and 7000 feet and between 7800 and 10,500 feet, in which TOC is frequently between 0.5 and 1.0 percent, with some values in excess of 1.0 percent (Flett, 1984). In the Mesozoic section of the COST No. 2 well, some samples containing carbonaceous siltstones and coal fragments exceed 1.0 percent TOC. The minimum TOC content required for oil generation is generally thought to be 0.5 percent (Hunt, 1979). Therefore, only a small portion of the sediments sampled in the COST wells is thought to have adequate organic carbon to be considered a possible source rock.

Kerogen Type

The organic matter in samples from the COST wells was analyzed petrographically and by pyrolysis to determine the types of kerogen present. In both COST wells, the petrographic analyses indicated relatively large amounts of humic (exinite) and herbaceous (vitrinite) kerogens, both of which are gas prone, and substantial amounts of inertinite, which has no hydrocarbon-generating potential. Amorphous material, an oil-prone kerogen presumably derived from algae, was present in relatively small amounts. Figure 19 illustrates the proportions of each kerogen type present in the COST No. 2 well.

Kerogen type and maturity of the COST No. 1 well samples were characterized by hydrogen-to-carbon (H/C) and oxygen-to-carbon (O/C) ratios based on the method of Tissot and others (1974). The results are plotted on a Van Krevelen diagram (fig. 20a) and indicate an

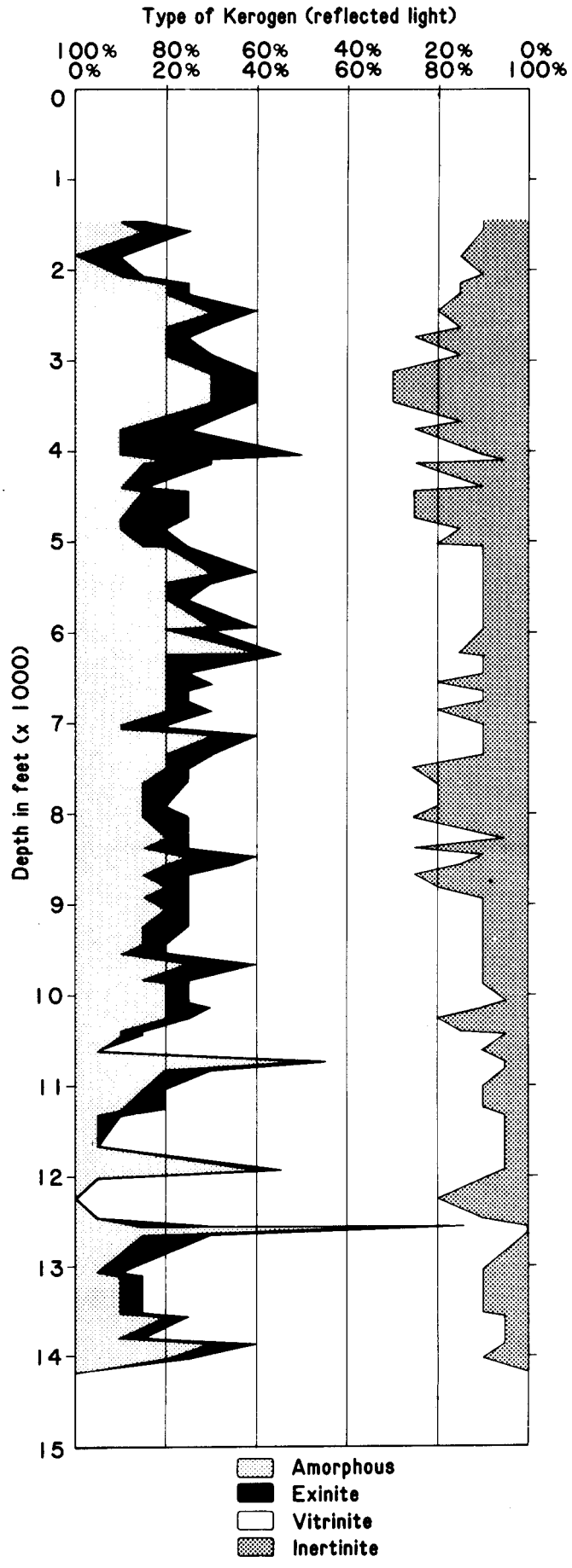

Figure 19. Percentage of kerogen types present in samples from the COST No. 2 well (Flett, 1984).

immature Type III kerogen. Type III kerogen is gas prone and is common in marine shelf sediments deposited in a well-oxygenated water column (Demaison, 1981). Elemental-analysis data are not available for the COST No. 2 well, but the pyrolysis data were used for the same type of classification based on the method of Espitalié and others (1977). The results are plotted on a modified Van Krevelen diagram (fig. 20b) and also indicate a Type III kerogen. The samples from 12,555 feet and 12,586 feet, which appear to fall in the oil-prone region, contained coal, which can cause a misrepresentation of kerogen type based on pyrolysis data (Peters, 1986). According to Flett (1984), there is no evidence that oil-prone Type I or Type II kerogen occurred in COST No. 2 well samples.

Thermal Maturation

The degree of thermal maturity attained by the sediments in the COST wells was measured in a variety of ways. Figure 21 displays four maturation indicators from the COST No. 2 well. These indicators include random vitrinite reflectance (R_o), kerogen fluorescence intensity, and spore coloration index, which are determined microscopically. Also included is T2-Max, the temperature at which maximum evolution of thermal hydrocarbons occurs, which is determined by pyrolysis. According to Flett (1984), the vitrinite reflectance is the most reliable of the indicators for this well. The data indicate that sufficient thermal maturity for peak oil generation (R_o = 0.6) is not attained until below about 12,400 feet. This depth is near the Cenozoic-Mesozoic boundary, which occurs at 12,540 feet. The thermal maturity data for the COST No. 1 well indicate a more shallow "oil window", beginning at about 4600 feet (Banet, 1984). However, this depth appears to be too shallow for the existing geothermal gradient (1.95°F/100 feet) and is inconsistent with data from the COST No. 2 well. The vitrinite reflectance data from the upper Tertiary section of the COST No. 1 well may be unduly influenced by recycled rather than primary vitrinite, which would give an artificially shallow oil window. Also, the vitrinite data populations are small for the COST No. 1 well because of the low TOC values, and this may make the data statistically imprecise (Banet, 1984). Therefore, the results from the COST No. 2 well are believed to provide a better indication of thermal maturity than those of the COST No. 1 well.

Potential in Other Areas

The sediments at the COST well sites are apparently unfavorable for oil generation based on the geochemical data. However, data from these two wells do not adequately test the potential for the entire St. George basin. The deepest part of the graben, north of the wells, contains more than 40,000 feet of Tertiary strata, whereas the thickest section encountered in the COST wells was less than 13,000 feet, encountered at the No. 2 well. It appears from the seismic profiles that the basal graben sediments were deposited in an enclosed basin when the area south of the graben, where the COST wells were drilled, was emergent. Restricted circulation in the early stage of graben development may have led to reducing

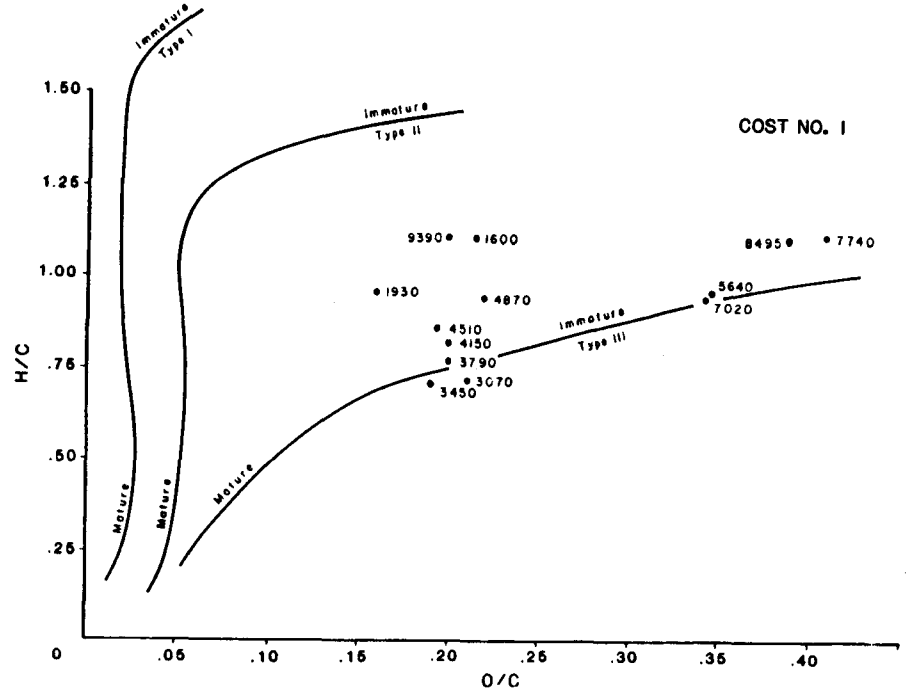

Figure 20A. Van Krevelen diagram (atomic ratios) for kerogens from the COST No. 1 well (Banet, 1984). Depths of samples given in feet.

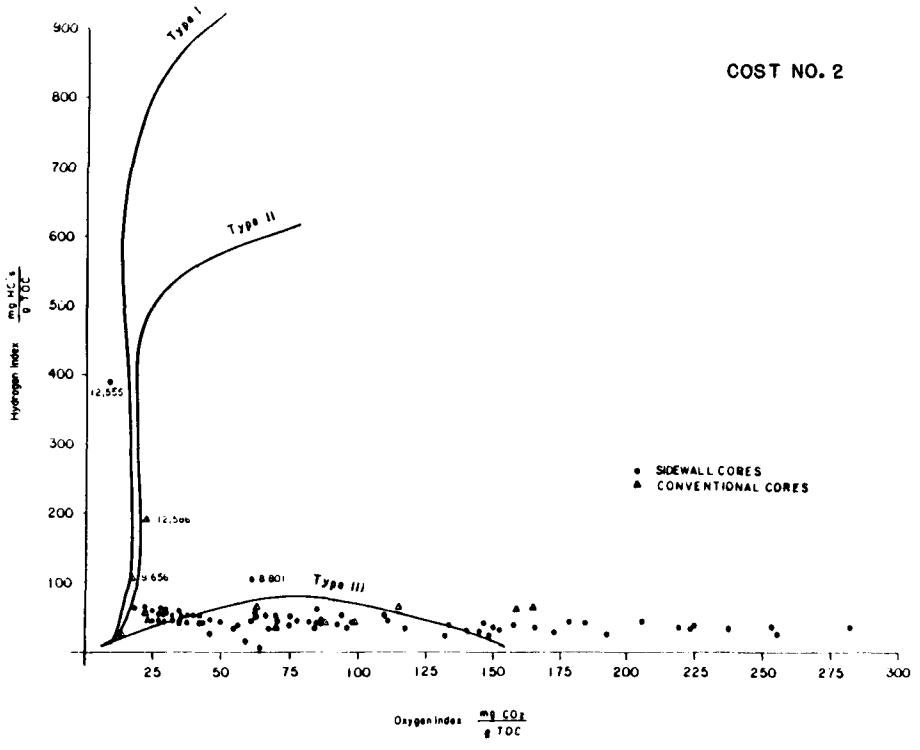

Figure 20B. Modified Van Krevelen diagram for kerogens from the COST No. 2 well (Flett, 1984). Depths of selected samples given in feet.

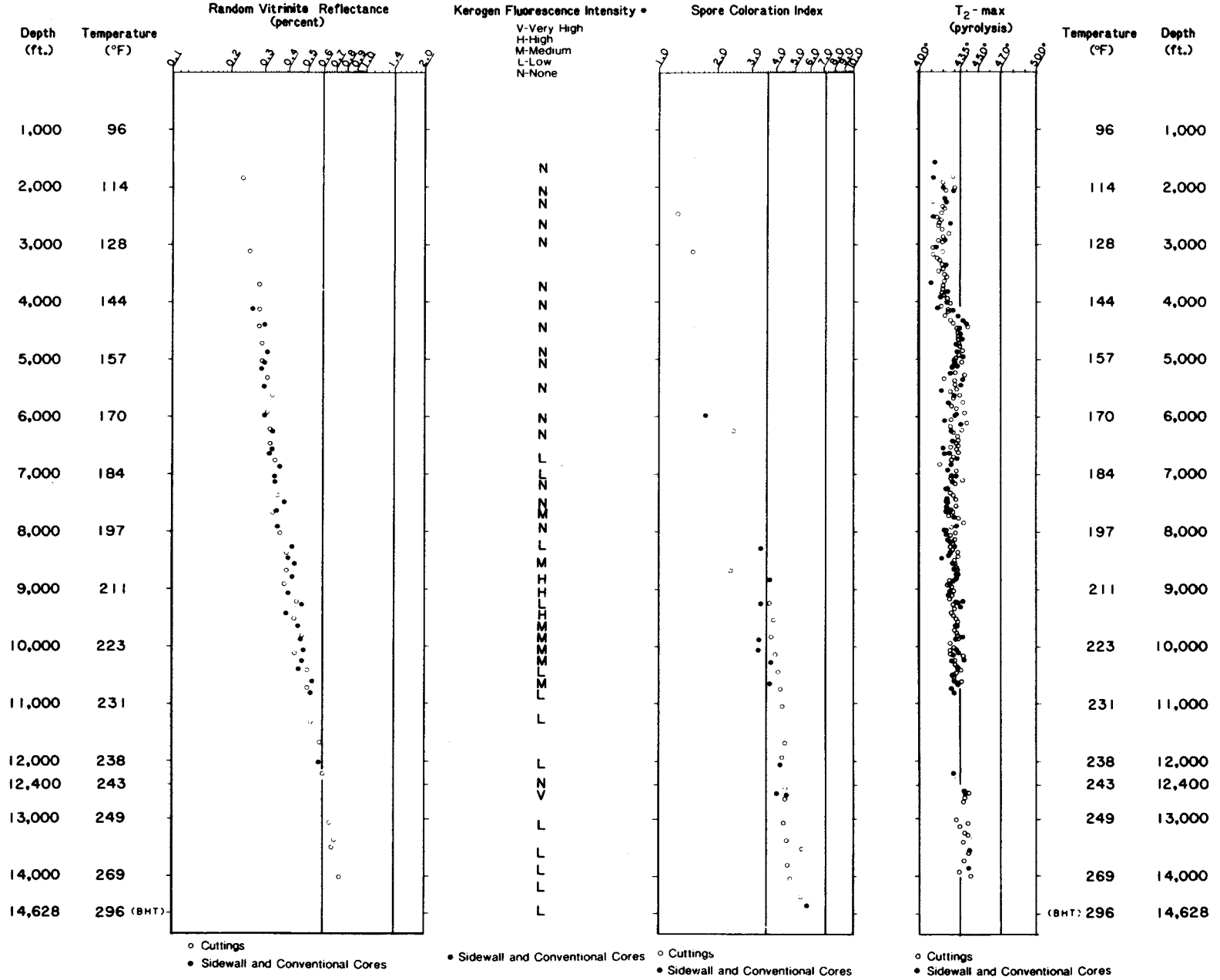

Figure 21. Thermal maturation indicators from the COST No. 2 well (Flett, 1984).

conditions, which would have been conducive to organic preservation. The geochemical characteristics of the basal graben sediments are unknown, but analogies are possible with Demaison's Type A or Type B organic facies, both of which are oil prone. Type A occurs in large anoxic lakes, such as Lake Tanganyika in the East African Rift Valley. Type B is an anoxic marine facies that occurs in some silled basins, such as the Black Sea (Demaison, 1981). The St. George graben, in its early stage of development, may have been a large rift valley lake or a marine silled basin. The potential for thermal maturity inside the graben is also more favorable than for the COST well locations because the basal graben sediments are buried more deeply than the lowermost Tertiary sediments at the COST well sites. Heat flow, moreover, was probably higher because of lithospheric extension in the graben. These sediments were probably exposed to high enough temperatures for a sufficiently long period of time to generate oil if oil-prone source rocks were present.

Source rock potential in the deep-water portion of the planning area is not well known. Some data are available from Deep Sea Drilling Project Hole 185, which was drilled along the flank of the Bering Canyon near the Umnak Plateau (Creager and others, 1973). Diatomaceous oozes and mudstones were recovered there to a depth of 728 meters, and the hole bottomed in probable upper Miocene sediments. Average TOC values were 0.5 percent, which is marginal at best (McIver, 1973).

TRAPS AND THE TIMING OF OIL MIGRATION

The types of traps likely to occur in the St. George graben include faulted anticlines, upthrown fault traps over basement horst blocks, downthrown fault traps along border faults of the graben, Tertiary strata draped over basement fault blocks, stratigraphic onlap of Tertiary sediments onto the basement, and possible stratigraphic pinch-out of sands. Subunconformity truncation traps may also exist below the ABU, although the Mesozoic rocks are too deep in many areas of the graben to be targets. The timing of trap development relative to possible hydrocarbon generation and migration in the St. George graben is probably favorable for accumulations to occur. The block-bounding faults are basement controlled and are associated with the structural collapse of the graben. Therefore, the structures existed well before potential source beds in the basal graben sediments would have become thermally mature.

In a study of hydrocarbon occurrences in grabens, Harding (1984) states that major accumulations are common in upthrown fault blocks and uncommon in downthrown blocks. The viability and capacity of the fault traps, especially on downthrown blocks, depends on whether or not the faults form effective seals to vertical migration of hydrocarbons. In the Niger delta, Weber and others (1978) note that reservoirs on downthrown fault traps were sealed only when overpressured zones occurred in the upthrown block across the fault plane. In the Louisiana Gulf Coast, Smith (1980) notes that fault seals commonly resulted from fault-zone materials, produced either

by mechanical or chemical processes. Detached listric faults are common in these two areas, and they usually have reverse drag or "rollover" traps on the downthrown block.

The St. George basin on the other hand has normal faults which are planar or only mildly listric. Rollover traps are rare; strata on the downthrown block are deformed by normal dip-slip drag along the fault instead. Normal drag causes the downthrown strata to dip away from the fault, which leaves the traps open to the faults. The downthrown strata in the graben are commonly juxtaposed against basement rocks (fig. 7b and fig. 11), which have virtually no permeability at the site of the COST No. 2 well or the Exxon wells (Y-0530 and Y-0527). Consequently, leakage of hydrocarbons across the fault plane into the upthrown block is improbable. Leakage up the fault plane, however, cannot be ruled out unless clay smearing or chemical precipitation seals the fault.

Stratal flexures in the Tertiary section associated with normal dip-slip drag may provide some closure on upthrown fault blocks, even for the case of nonsealing faults. Sealing faults, however, would permit the traps to fill to a greater capacity.

On the shelf outside the graben, potential traps are found both above and below the acoustic basement unconformity. Recognized traps below the acoustic basement unconformity include antiformal structures and subunconformity truncation. The subunconformity plays directly underlie the unconformity that separates the well-stratified section from the acoustic basement. Traps above the acoustic basement unconformity include anticlinal structures resulting from drape of Tertiary sediments over basement highs, fault-bounded closures, and stratigraphic onlap of Tertiary sediments onto basement highs.

The time at which the rocks constituting the acoustic basement reached thermal maturity is not known. Therefore, it is not known whether the structures seen within acoustic basement formed before or after hydrocarbon migration would have occurred. If migration did not occur until after the middle Eocene to early Oligocene, trapping could have occurred both within the basement antiformal structures and at the subunconformity truncation. The Mesozoic rocks at the COST No. 2 well are not overmature for oil generation, so early migration is unlikely. Traps within the well-stratified section appear to have formed syndepositionally, and thus could have begun collecting hydrocarbons once overlying seals had formed. For example, the Oligocene reservoir rocks would be filled only if migration occurred during the Miocene or later. In addition to possible source rocks from within the acoustic basement, hydrocarbons may have migrated from the graben along the bounding faults and into Oligocene sands in traps proximal to the graben.

In the Pribilof basin, potential traps include basement anticlines with drape in the overlying Tertiary section, upthrown fault traps over tilted basement blocks, and subunconformity truncation associated with fault-bounded anticlines. The timing of

trap development should be favorable because these structures formed early in the basin history. It is not known, however, if adequate source beds exist within the basin or whether such beds are thermally mature.

In the deep-water area, potential traps include stratigraphic pinch-outs, turbidite sands interbedded with hemipelagic mud, lateral diagenetic variations, diapirs (Scholl and Marlow, 1970), and fault-bounded traps.

EXPLORATION HISTORY

St. George Basin Lease Sale 70 was held on April 12, 1983, and leases were issued on March 1, 1984. Of the 479 tracts offered, bids were accepted on 96 tracts and rejected on 1. Winning bids totaled $426 million, with the highest bid being $36.6 million. Nine exploratory wells have been drilled on these leases, all during the 1984-1985 drilling season. All of these holes have been plugged and abandoned.

Drilling locations are shown in figure 22. Four of the holes were located within the graben and the remaining five were located south of the graben. Chevron drilled an 11,595-foot well (lease number Y-0519) in the graben. Exxon drilled two holes in the graben, the first to 8800 feet (Y-0530), the second to 12,433 feet (Y-0527). ARCO drilled a vertical hole to 10,860 feet in the graben (Y-0511), and then drilled a sidetrack hole from approximately 5000 feet to 13,937 feet (measured depth). ARCO also drilled a 12,456-foot hole south of the graben (Y-0537). Gulf has drilled one hole to a depth of 9592 feet (Y-0477). Mobil drilled an 8085-foot hole (Y-0466) near the boundary of the North Aleutian Basin Planning Area. The remaining two holes were drilled by Shell, one to 10,277 feet (Y-0454) and the other to 8510 feet (Y-0463).

EXXON WELLS

Data from the two Exxon wells are now publicly available because the leases were relinquished by the company. These wells were drilled on a horst block in the center of the graben. The first well (Y-0530) was drilled on the crest of the structure to 8800 feet (all depths are below kelly bushing, 89 feet above sea level). According to Exxon's completion report, the well encountered the top of the Pliocene at 1850 feet, the late Miocene at 4160 feet, the Oligocene at 6910 feet, and the Late Jurassic at 7200 feet. Pliocene and Miocene sediments consist of sandy siltstones and very fine to fine-grained silty sandstones with abundant fossil fragments. Oligocene lithologies are very similar at the top, grading downward into a well-cemented, gray calcareous conglomerate from 7165 to 7200 feet, which is the base of the Tertiary. The basal conglomerate overlies a hard gray calcareous siltstone of Jurassic age. The remainder of the Jurassic section consists of calcareous shale, silty

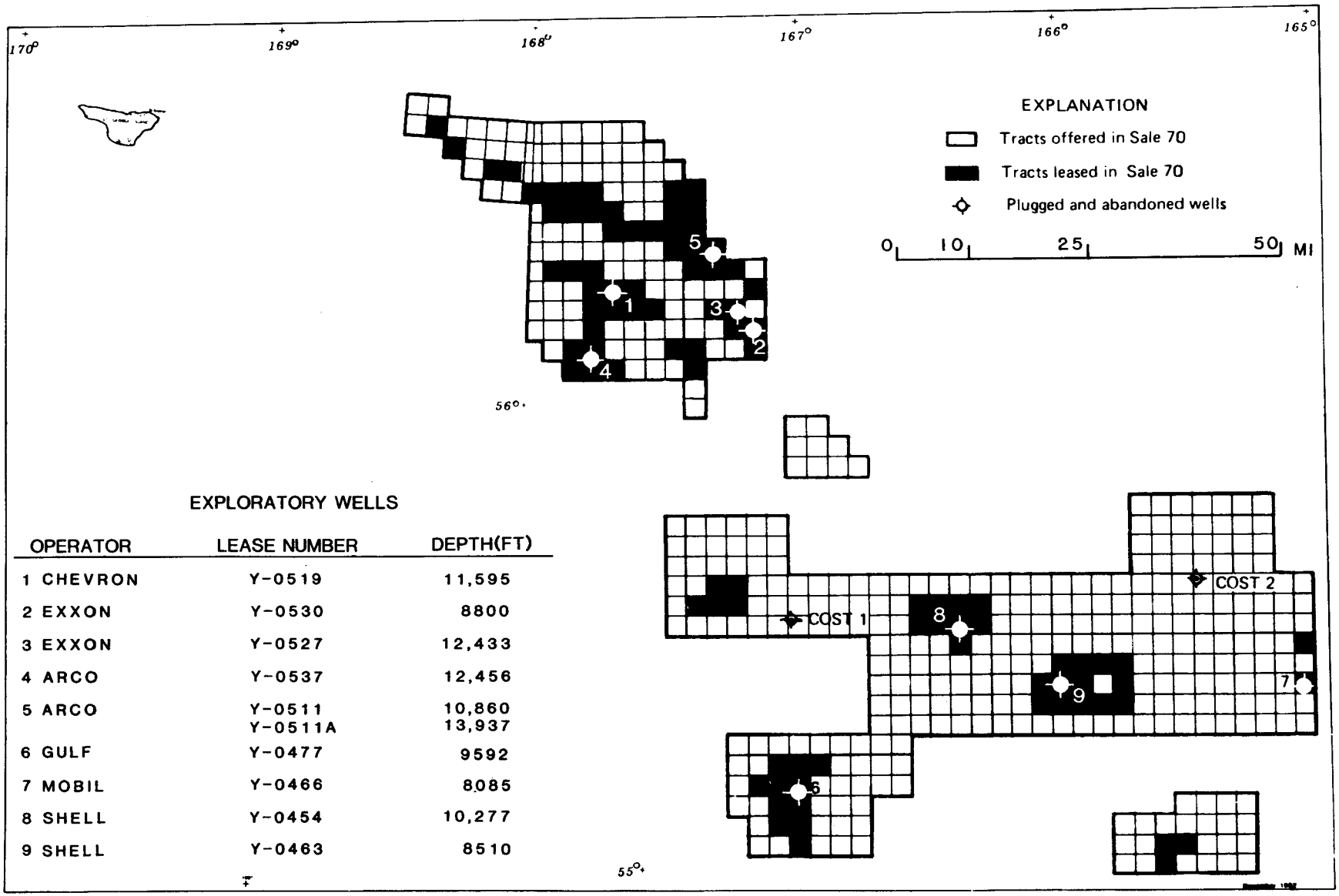

EXPLORATORY WELLS

OPERATOR	LEASE NUMBER	DEPTH(FT)
1 CHEVRON	Y-0519	11,595
2 EXXON	Y-0530	8800
3 EXXON	Y-0527	12,433
4 ARCO	Y-0537	12,456
5 ARCO	Y-0511	10,860
	Y-0511A	13,937
6 GULF	Y-0477	9592
7 MOBIL	Y-0466	8085
8 SHELL	Y-0454	10,277
9 SHELL	Y-0463	8510

Figure 22. Location of COST wells and exploratory wells in the St. George Basin Lease Sale 70 area through 1986.

sandstone, and sandy siltstone. Reservoir rock potential is apparently poor throughout the Cenozoic and Mesozoic section.

Seismic interval velocities derived from the well velocity survey average about 8200 feet/second for the Miocene section and about 9000 feet/second for the Oligocene section above the basal conglomerate. These values compare closely to those of the COST wells for equivalent-age sediments at comparable burial depths (fig. 13). The interval velocity increases abruptly to about 14,000 feet/second in the basal conglomerate, and the Jurassic rocks average about 14,600 feet/second. These values fall outside the range for normal compaction in the basin. These velocities are not high compared to those of the COST No. 2 Mesozoic section, but the rocks are approximately 5000 feet more shallow at the Exxon site. Also, the Mesozoic rocks at Exxon's second well (Y-0527) have lower interval velocities, even though they are about 3000 feet deeper. This implies that the Upper Jurassic rocks and possibly the basal Tertiary conglomerate at the crest of the horst were deeply buried, compacted, and subsequently uplifted.

The first Exxon well was located over a seismic acoustic anomaly that indicated the presence of gas in the sediments. This anomaly was apparent on both shallow, high-resolution profiles and deep MCS data. Seismic reflections are discontinuous and incoherent over the crest of the structure, and velocity pull-down occurs where coherent reflections grade laterally into the acoustically turbid zone. The well encountered gas dispersed in the sediment at shallow depth and at several zones throughout the Cenozoic section, including the basal conglomerate. Dispersed gas proved to be an engineering problem after 20-inch conductor casing was set and cemented at 1474 feet. Gas bubbles were observed emanating from the annulus between the conductor and the structural casing. Bubbling was monitored with subsea television for 8 hours, and drilling resumed to 2563 feet after the gas appeared to be depleting. The bubbling continued, however, and the well was plugged back and recemented. No further problems resulted from gas, but 6 days of rig time were lost. Abnormally high formation pressures were not encountered, but gas-cut mud was a problem.

A drill stem test was conducted from 7167 to 7210 feet in the basal Tertiary conglomerate and upper 10 feet of Jurassic sediments. The well flowed salt water and a small amount of gas. The tool was open for 17 hours and 21 minutes, and 145 barrels of water were recovered at an average rate of 175 barrels per day.

Exxon's second exploratory well (Y-0527) was drilled on the flank of the horst to a depth of 12,433 feet (below kelly bushing, 86 feet above sea level). The well reportedly encountered the top of the Pliocene at 2060 feet, the Miocene at 4430 feet, the Oligocene at 8900 feet, and pre-Tertiary sediments at 10,470 feet. Pliocene sediments consist of clayey siltstones, silty clays, and minor sands. Miocene lithologies are similar, but very fine silty sandstones are common to about 6600 feet. They are rare below this depth. Argillaceous lithologies also predominate in the upper Oligocene

section, from 8900 to 9270 feet. From 9270 to 10,000 feet, the section consists of sandstones interbedded with siltstones. As measured on the SP log, the sand beds range from 5 to 20 feet in thickness for a gross total of 185 feet. The sands are very fine to fine grained, sometimes silty, and reportedly contain volcanic lithic fragments. At the base of the Tertiary section, the mud log describes gray to green volcanics from about 10,100 to 10,470 feet, while the sidewall core description reports silicified volcaniclastic sediments. These rocks are denser (about 2.6 g/cm^3) than the overlying or underlying sediments, and they may be pyroclastics that are interbedded with volcaniclastic sediments. The pre-Tertiary section, from 10,470 to 12,433 feet, is predominantly siltstone with carbonaceous mudstone, minor sandstone, and some coal. According to both the mud log and the sidewall core description, these sediments appear slightly metamorphosed. Reservoir rock potential is apparently poor throughout the well with the possible exception of the sands from the lower Oligocene interval, which may have fair potential.

Seismic interval velocities average about 8800 feet/second in the Miocene section, about 10,000 feet/second in the upper Oligocene argillaceous section, and about 11,000 feet/second in the lower Oligocene sandy section. These values are consistent with the COST well data for comparable age sediments at similar depths (fig. 13). Velocities increase abruptly to about 13,800 feet/second in the volcanic(?) section, which is slightly lower than the basalt interval velocities measured in the COST No. 1 well. Velocities decrease slightly to about 13,600 feet/second in the underlying pre-Tertiary section, but the well velocity survey terminates at 10,761 feet, so data are not available for the deeper Mesozoic section extending to 12,433 feet.

3. Environmental Geology

The area of highest petroleum potential in the St. George Basin Planning Area occurs on the outer continental shelf in water depths between 100 and 200 meters. The sea floor is essentially flat and featureless between the 100- and 200-meter isobaths, with an average regional slope of less than 1^{o}. The shelf edge is incised by two large submarine canyons, the Pribilof Canyon and the Bering Canyon. The walls of the canyons and the continental slope show evidence of mass sediment movement.

Potential geologic hazards in the planning area include unstable slopes, shallow gas, shallow faults, seismicity, and volcanism. Other environmental constraints are associated with the harsh climate, such as pack ice, storm waves, and superstructure icing on drilling rigs and supply boats. The climatic factors have been reported elsewhere (Hood and Calder, 1981), and the geologic hazards are discussed below.

NEAR-SURFACE SEDIMENTS

According to Gardner and others (1980), the surficial sediments of the outer Bering shelf consist mostly of unconsolidated silt and silty sand, with low concentrations of volcanic ash and diatoms, and are mostly relict from a period of low sea level. Very little recent sediment is being transported into the area. A geotechnical corehole drilled to 72 meters below mudline at the COST No. 1 well recovered sediments that were Pleistocene in age except for a thin veneer of Holocene sediments at the surface. Lithologies ranged from silty clays to fine silty sands. The surficial 2 meters of sediments (Holocene?) were soft and of medium to low plasticity; the underlying sediments were much stiffer and had higher plasticity and shear strength (Woodward-Clyde Consultants, 1976).

UNSTABLE SLOPES

Gardner and others (1979) recognized potentially unstable sediment masses on the continental slope and in the submarine canyons of the Bering shelf margin. The types of slope failure that occur include gravity slides, slumps, and creep. The features indicative of slope failure recognized by Gardner and others (1979) on high-

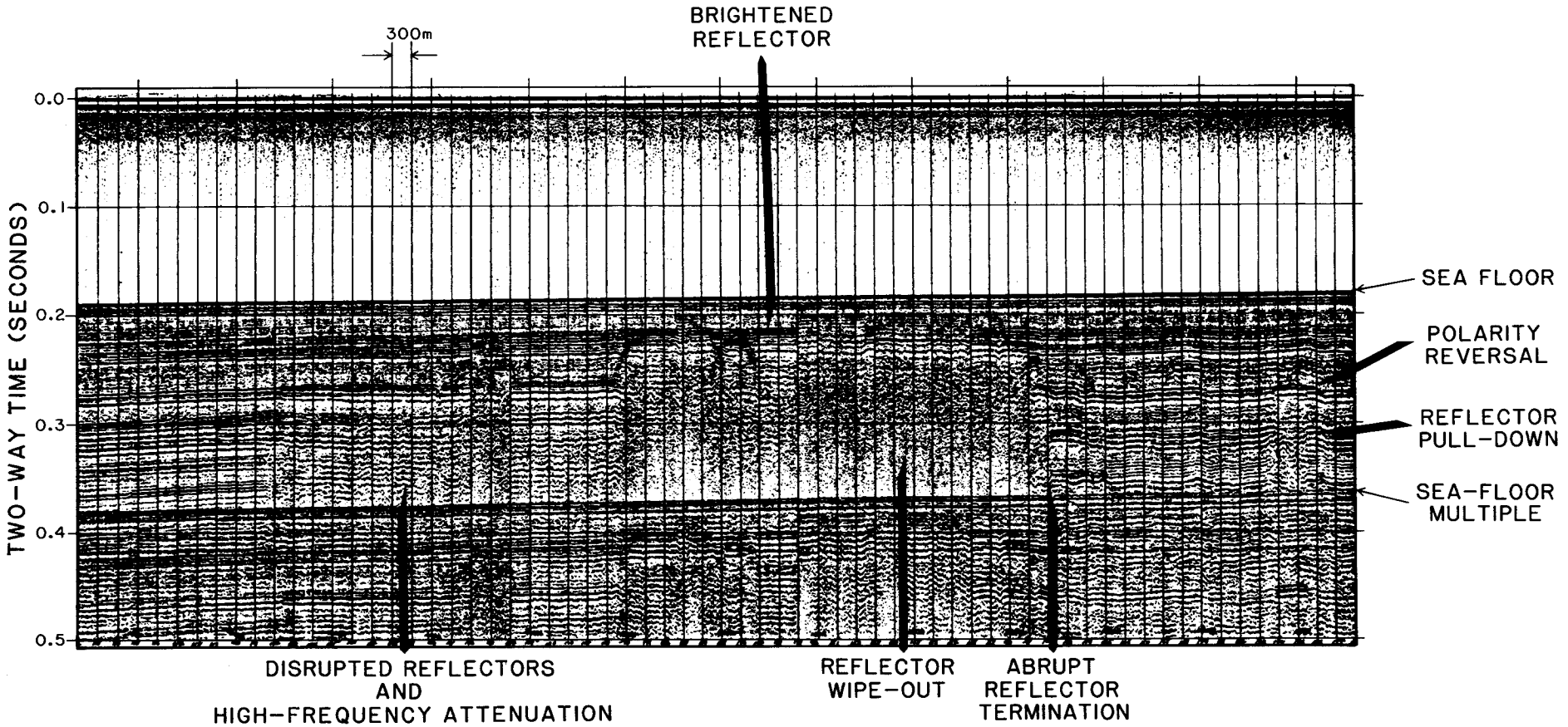

Figure 23. High-resolution seismic reflection profile illustrating the types of acoustic anomalies inferred to indicate shallow gas in the St. George basin (Comer, 1984a).

resolution seismic profiles include surface faults with steep scarps and rotated surfaces, deformed bedding and discontinuous acoustic reflections, hummocky topography, anomalously thick sediment accumulations, and acoustically transparent sediment masses. Most areas along the continental slope and the walls of the submarine canyons are potentially unstable. Slope failure will not be hazardous to exploratory wells drilled in these areas from floating platforms, but may be hazardous to bottom-founded production platforms and pipelines.

SHALLOW GAS

Hydrocarbon gas in marine sediments may occur as gas-charged sediment or confined gas accumulations. Gas-charged sediments contain normally pressured gas dispersed throughout surficial sediments and usually occur over broad areas. Confined gas accumulations are localized in structural or stratigraphic traps at any subbottom depth and may be abnormally pressured. The presence of shallow gas in St. George basin has been inferred from acoustic anomalies on seismic reflection profiles, and has been confirmed in drill holes. Kvenvolden and others (1981) reported small quantities of hydrocarbon gas in shallow sediment cores (less than 2 meters). Dispersed gas was reported in the 236-foot (72-meter) geotechnical corehole drilled at the COST No. 1 well site and in an Exxon exploratory well (Y-0530).

Shallow, gas-charged sediments have a lower shear strength and bearing capacity than normal sediments, and are also more susceptible to pore-pressure fluctuations and liquefaction due to cyclic loading, as might be initiated by earthquakes or long-period storm waves. For these reasons, engineering considerations for bottom-founded structures or equipment installed on the sea floor are more important in areas underlain by gassy sediments. Shallow gas under normal pressure poses less of a hazard than confined gas accumulations, which may be abnormally pressured. Confined, high-pressure gas may cause a well blowout if penetrated unexpectedly during drilling operations unless adequate precautions are taken.

Figure 23 is a high-resolution, seismic reflection profile that illustrates the types of acoustic anomalies occurring in the planning area that are attributed to shallow gas. The areal distribution of these anomalies was mapped by Comer (1984a). These features are very common in the St. George graben and on the continental shelf south of the graben. They are rare to absent in the Pribilof basin and uncommon on the slope and in the deep-water parts of the planning area.

No active gas seeps in the water column are evident on the seismic profiles collected for geologic-hazards mapping. Sea-floor pockmarks are apparent on side-scan sonographs and bathymetric records, however. In each case, these features are underlain by acoustic anomalies, suggesting that they may be gas craters formed by periodic release of interstitial gas from the surficial sediment.

Exxon's first exploratory well (Y-0530) was located over a gas anomaly which disrupted seismic reflections on both shallow, high-resolution profiles and deep MCS data. Dispersed gas was encountered at shallow depth and at several zones throughout the well. Although the gas was not abnormally pressured, it did prove to be a costly engineering constraint (the drilling operations are described in the Exxon Wells section, this report).

Most of the acoustic anomalies that blanket large areas of the St. George basin are probably caused by biogenic gas-charged sediments. These areas may pose little risk of blowouts, but differentiating them from areas of more hazardous, over-pressured gas accumulations is difficult using only regional seismic data. Hazards posed by shallow gas must be evaluated case by case using data collected specifically for hazards evaluation of a drill site.

SHALLOW FAULTS

Faults which displace strata within 100 meters of the sea floor in the St. George basin were mapped by Comer (1984a). These faults generally trend northwest-southeast, parallel to the axis of the St. George graben. They are high-angle normal faults and have increasing offsets with depth on the downthrown block, indicating that subsidence and fault movement have been contemporaneous with deposition. Border faults along the margin of the graben often intersect the sea floor, and sea-floor offsets of 1 to 2 meters are apparent on some seismic reflection profiles (fig. 24). Shallow faults in the planning area are most common along the margin of the graben. They occur in the Pribilof basin, but are very rare elsewhere in the planning area except for detached surface faults associated with slumps on the continental slope.

SEISMICITY

The St. George basin is located in a seismically active region. During the period 1925-1978 there were four earthquakes in that area with magnitudes greater than 6.0 on the Richter Scale (7.20 in 1925, 6.75 in 1941, 6.38 in 1958, and 6.50 in 1959)(Davies, 1981). Figure 25 shows the location of epicenters of the earthquakes during this period.

A large number of shallow focus earthquakes (depth$\leq$110 km) have occurred in the vicinity of the St. George basin. These earthquakes are probably associated with faulting in the St. George graben, but this assumption cannot be confirmed with the presently available data (Davies and Jacob, 1981). Many of the earthquake epicenters to the south and east of the St. George basin, near the Aleutian Islands and the Alaska Peninsula, are deep focus (depth$\geq$110 km). These occur along the Wadati-Benioff zone beneath the Aleutian arc and are caused by subduction of the Pacific plate beneath the arc.

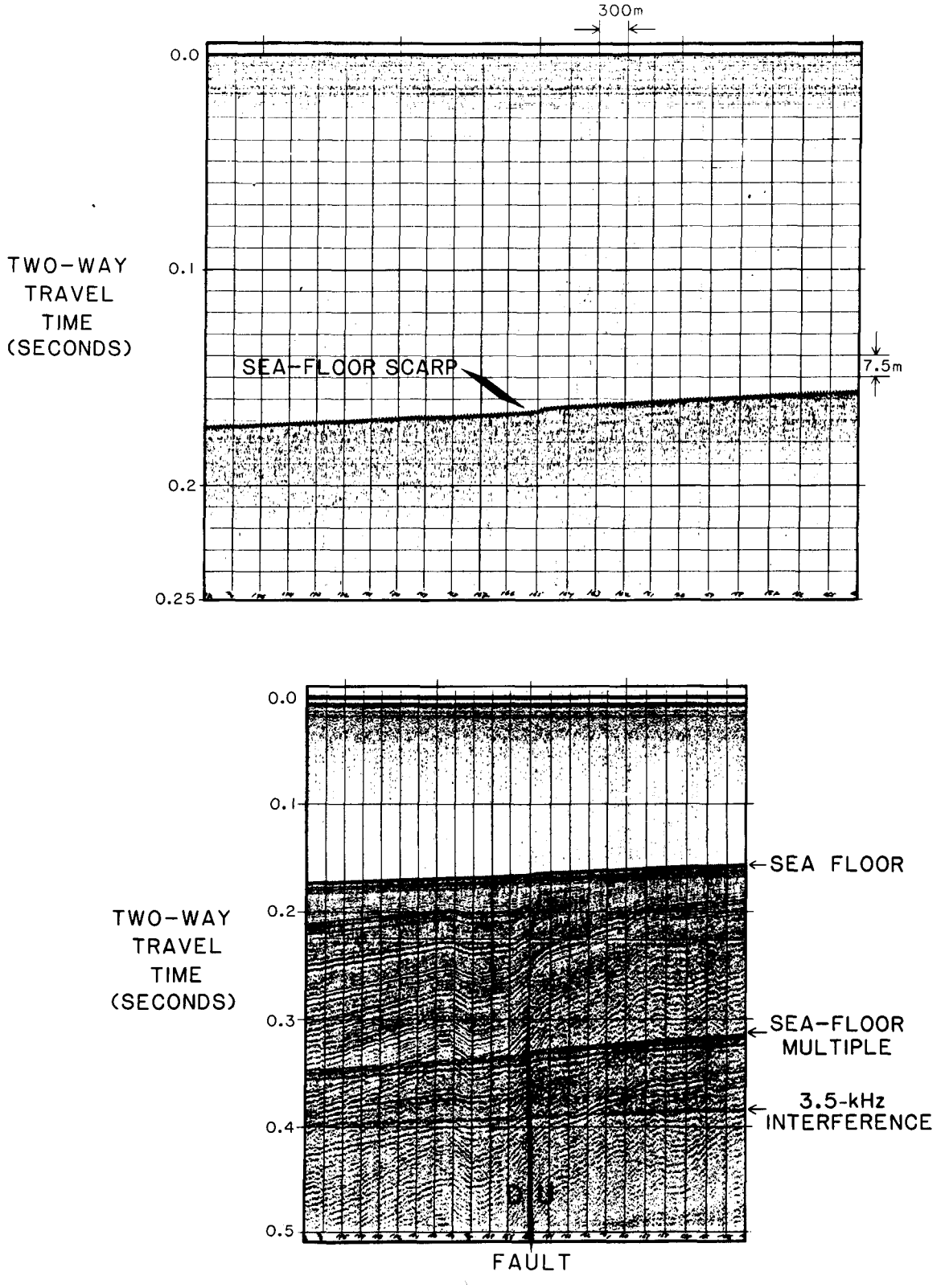

Figure 24. (Top section) 3.5 - kHz subbottom profiler record showing a fault scarp on the sea floor in the St. George basin. (Bottom section) 1000 - Joule analog-sparker record of same line showing fault that displaces sea floor.

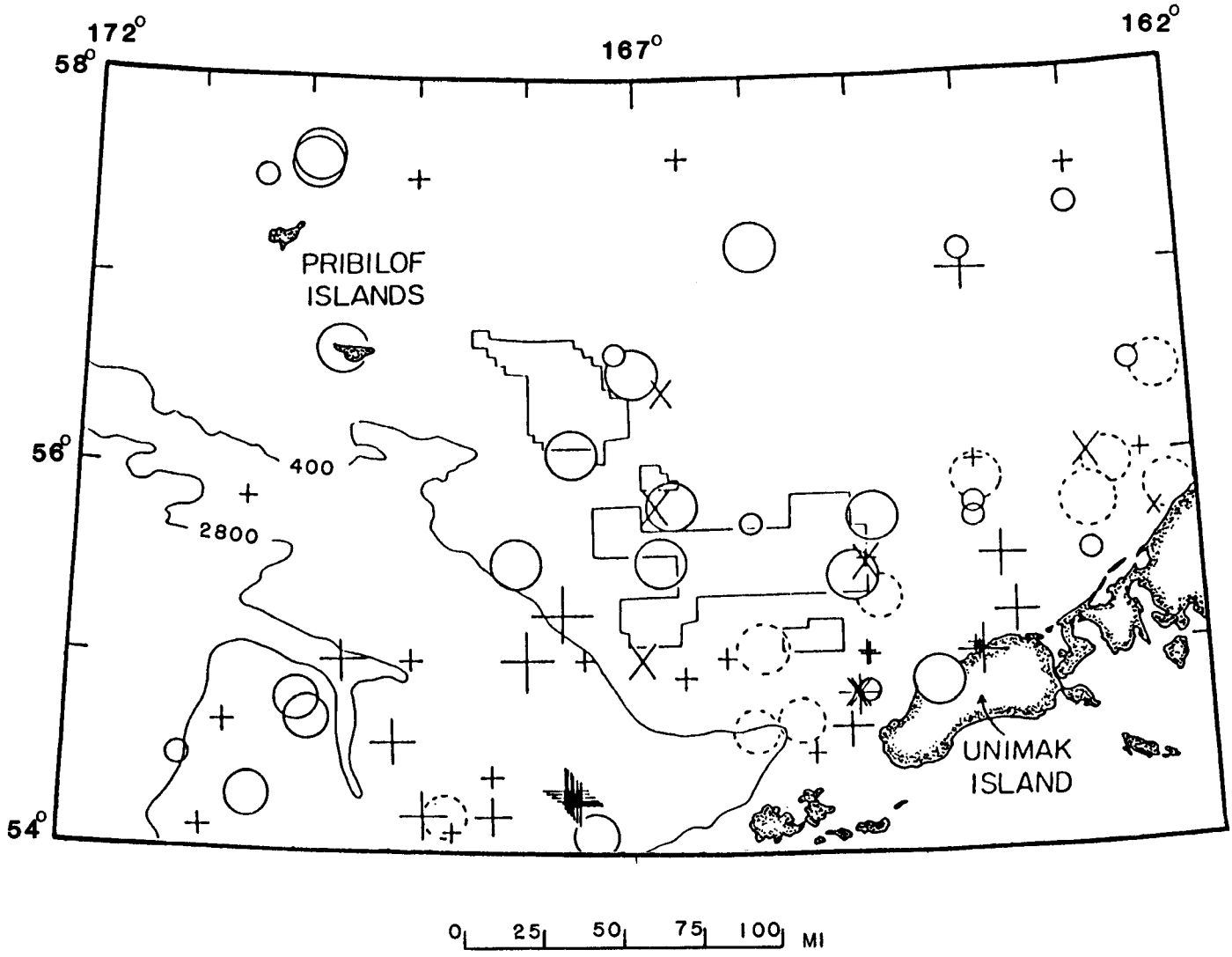

Figure 25. Earthquake epicenters, greater St. George basin area, 1925 through 1978. Epicenter symbols are scaled by magnitude. Crosses represent events with unknown depths; x's, those inferred to be shallow; solid circles, those known to be shallow (< 75 km); dashed circles, those known to be deep (> 113 km) (Davies, 1981).

It is expected that earthquakes will continue to be hazardous in the St. George area. Davies (1981) predicted a maximum magnitude in the vicinity of the St. George graben of about 8.0. Based on the earthquake record from 1957 through 1978, Davies calculated that the probability that ground shaking would exceed 0.2-g acceleration within a 40-year interval at a randomly chosen site is about 11 percent, and the probability for acceleration exceeding 0.5 g is about 3 percent. In the Aleutian Islands and the Alaska Peninsula, the seismic risk is greater, particularly in areas between aftershock zones of previous major earthquakes, called seismic gaps by Sykes (1971). The Shumagin gap south of the Alaska Peninsula (162° to 159° W) is one such area (Davies, 1981), and the Unalaska gap (167° to 164° W) may be a second (House and Boatwright, 1980) (fig. 26). Both areas have the potential to produce a single earthquake of magnitude greater than 8.7, or a series of earthquakes greater than 7.8 (Davies, 1981). The potential seismic risk from these very large earthquakes is greatest in the southeastern portion of the St. George Basin Planning Area.

Earthquakes will probably not cause a severe hazard during exploration because drilling will be done from floating platforms such as drill ships or semi-submersibles. During production, platforms may be bottom supported, so there could be some risk at this stage. The greatest hazard will be to onshore facilities. The siting and design of support facilities on the Aleutian Islands and the Alaska Peninsula should take into account the high seismic risk there, particularly within the Shumagin and Unalaska seismic gaps.

VOLCANISM

The Aleutian arc, one of the most volcanically active areas in the world, bounds the St. George Basin Planning Area on the south. Fifteen active volcanoes are located within or near this area (fig. 26). Davies (1981) assessed the potential of these volcanoes to erupt at any given time based on the records of historical activity (table 2). Eight have a high potential to erupt, one moderate, and the remaining six low. As there may be a correlation between the length of time between eruptions and their severity, even those with low potential must be considered hazardous.

The volcanoes in the Aleutian arc are andesitic and therefore tend to erupt explosively. Although the direct blast poses the most severe threat, ash flows may also be a hazard. Studies on the Alaska Peninsula (Miller and Smith, 1977) show that ash flows have traveled across lowlands (35 meters elevation) and then up through 260-meter passes, traveling a total distance of 50 kilometers. There is also evidence of an ash flow crossing a barrier 500 meters high (Miller and Smith, 1977). Mud slides and flash floods generated by rapid snow melt are other potential hazards to onshore facilities associated with volcanic eruptions (Davies, 1981).

The Pribilof Islands, northwest of St. George basin, are another site of potential volcanism. Eruptions on the islands have

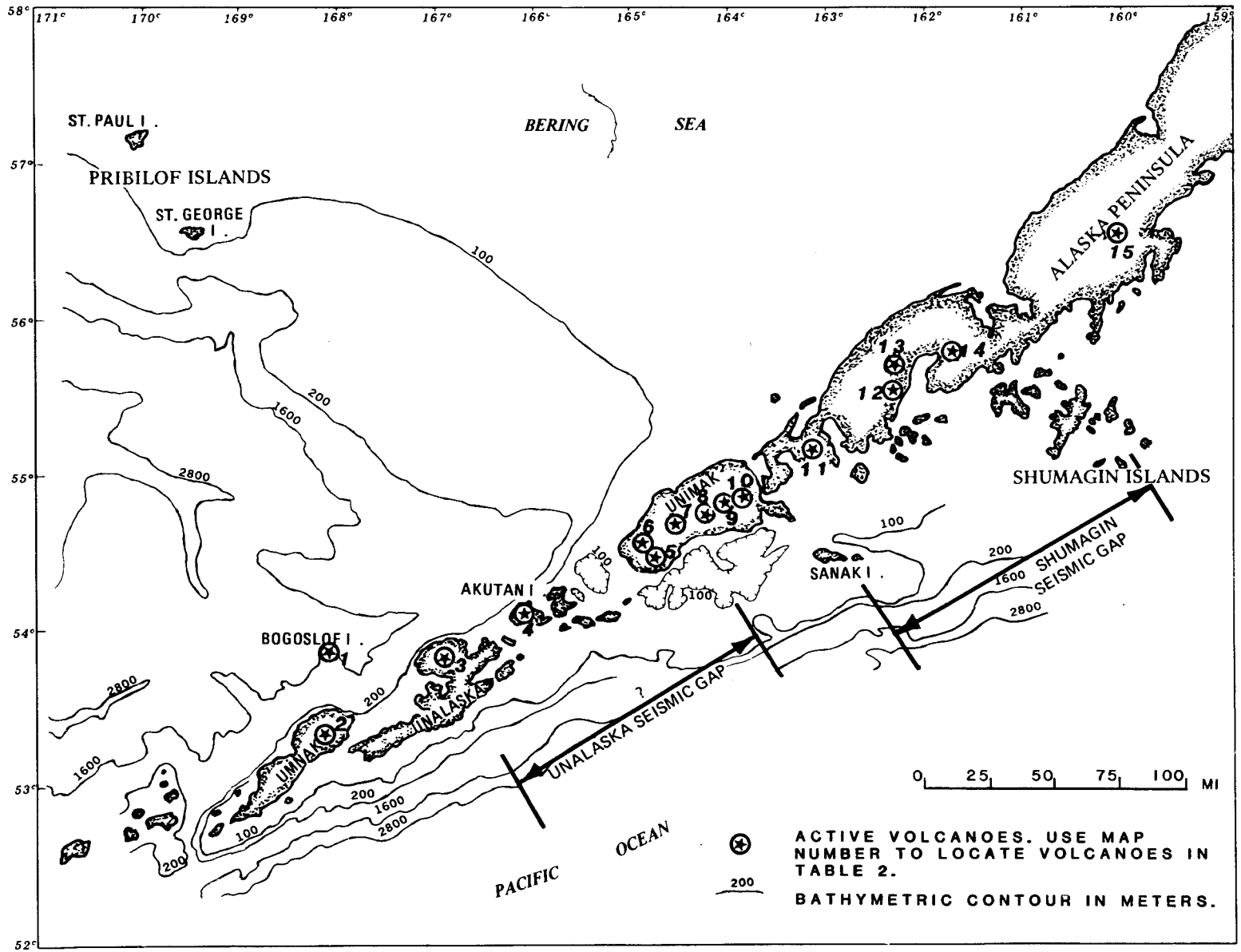

Figure 26. Active volcanoes near the St. George basin. Numbers correspond to volcanoes listed in table 2 (FEIS, Sale 70).

TABLE 2. Active volcanoes in the vicinity of the southern boundary of Sale 70.

Map No.[1]	Name	Potential for Eruption[2]	Type of Eruption	Date of Last Eruption
1	Bogoslof	High	Normal Explosion	1931
2	Okmok	High	Normal Explosion, Lava	1945
3	Makushin	High	Normal Explosion	1938
4	Akutan	High	Normal Explosion, Lava	1973
5	Westdahl	High	Normal Explosion, Lava	1967
6	Progromni	High	Normal Explosion, Lava	1830
7	Fisher	Low	Ash	1826
8	Shishaldin	High	Lava	1975-76
9	Isanotski Peaks	Moderate	Normal Explosion, Ash	1845
10	Roudtop Mt.	Low	-----	----
11	Frosty Peak	Low	-----	----
12	Pavlof	High	Normal Explosion, Lava	1975-76
13	Pavlof Sister	Low	Ash	1786
14	Dana	Low	-----	----
15	Veniaminaf	Low	Normal Explosion, Ash	1944

Source: U.S. Minerals Management Service, 1982

1. Number refers to figure 26.
2. Based on historic activity.

not been reported since the early 1800's and are thought to be unlikely in the future (Davies, 1981). These islands are formed by basaltic lava, so any future eruptions are not expected to be explosive and therefore should have only local effects.

TSUNAMIS

There have been 54 recorded occurrences of tsunamis or seiches produced by earthquakes in Alaska (Meyers, 1976). Many of these caused loss of life or property. The high probability of earthquakes in the Aleutian Islands and the Alaska Peninsula makes tsunamis a threat to support facilities there. A major earthquake near the Shumagin Islands could generate tsunami heights of about 30 meters on the Pacific shores of the Aleutian Islands. Volcanic eruptions could cause local tsunamis that may travel distances of 100 to 150 kilometers (Davies, 1981).

References

AGAT Consultants, Inc., 1982, Reservoir quality study, ARCO St. George Basin COST Well No. 2: Denver, 5 v. Independent consultant report prepared for ARCO Exploration Company.

Banet, A. C., 1984, Organic geochemistry, in Turner, R. F., ed., Geological and operational summary, St. George Basin COST No. 1 well, Bering Sea, Alaska: U.S. Minerals Management Service OCS Report MMS 84-0016, p. 79-92.

Bolm, J. G., 1984a, Lithology and well log interpretation, in Turner, R. F., ed., Geological and operational summary, St. George Basin COST No. 1 well, Bering Sea, Alaska: U.S. Minerals Management Service OCS Report MMS 84-0016, p. 41-78.

Bolm, J. G., 1984b, Lithology and well log interpretation, in Turner, R. F., ed., Geological and operational summary, St. George Basin COST No. 2 well, Bering Sea, Alaska: U.S. Minerals Management Service OCS Report MMS 84-0018, p. 38-72.

Brockway, R., Alexander, B., Day, P., Lyle, W., Hiles, R., Decker, W., Polski, W., and Reed, B., 1975, Bristol Bay region "stratigraphic correlation section" southwest Alaska: Anchorage, Alaska Geological Society, 1 oversized sheet.

Brown, C., and Girdler, R. W., 1980, Interpretation of African gravity and its implications for the breakup of continents: Journal of Geophysical Research, v. 85, p. 6443-6445.

Burk, C. A., 1965, Geology of the Alaska Peninsula island arc and continental margin: Geological Society of America Memoir 99, 250 p.

Childs, J. R., Cooper, A. K., and Parker, W. A., 1979, Sonobuoy studies of the Umnak Plateau, Bering Sea [abs.]: EOS (Transactions of the American Geophysical Union), v. 60, p. 390.

Childs, J. R., Cooper, A. K., and Wright, A. W., 1981, Residual magnetic map of Umnak Plateau, Bering Sea [abs.]: EOS (Transactions of the American Geophysical Union), v. 60, p. 390.

Cochran, J. R., 1983, A model for the development of the Red Sea: AAPG Bulletin, v. 67, p. 41-69.

Comer, C. D., 1984a, Map showing shallow faults and acoustic anomalies, St. George Basin, Alaska: U.S. Minerals Management Service OCS Map MMS 84-0012, 1 oversized sheet, scale 1:250,000.

Comer, C. D., 1984b, Seismic reflection correlation and velocity analysis, in Turner, R. F., ed., Geological and operational summary, St. George Basin COST No. 2 well, Bering Sea, Alaska: U.S. Minerals Management Service OCS Report MMS 84-0018, p. 11-12.

Cooper, A. K., Marlow, M. S., Parker, A. W., and Childs, J. R., 1979b, Structure-contour map on acoustic basement in the Bering Sea: U.S. Geological Survey Miscellaneous Field Studies Map MF-1165, 1 oversized sheet, scale 1:2,500,000.

Cooper, A. K., Marlow, M. S., and Scholl, D. W., in press, Geologic framework of the Bering Sea crust, in Scholl, D. W., Grantz, A., and Vedder, J., eds., Geology and resource potential of the continental margin of western North America and adjacent ocean basins--Beaufort Sea to Baja California: AAPG Memoir, Tulsa.

Cooper, A. K., Marlow, M. S., and Vallier, T. L., 1984, Summary geologic report for the St. George OCS planning area, Bering Sea, Alaska: U.S. Geological Survey Open-File Report 84-418, 81 p.

Cooper, A. K., Scholl, D. W., Marlow, M. S., Childs, J. R., Redden, G. D., Kvenvolden, K. A., and Stevenson, A. J., 1979a, Hydrocarbon potential of the Aleutian Basin, Bering Sea: AAPG Bulletin, v. 63, p. 2070-2087.

Cooper, A. K., Scholl, E. W., Vallier, T. L., and Scott, E. W., 1980, Resource report for the deep water areas of proposed OCS Lease Sale No. 70, St. George Basin, Alaska: U.S. Geological Survey Open-File Report 80-246, 91 p.

Core Laboratories, Inc., 1976, Core analysis report for ARCO Alaska, Inc., St. George Basin COST No. 1 well stratigraphic test, St. George Basin, Alaska: Dallas.

Cox, A., Hopkins, D. M., and Dalrymple, G. B., 1966, Geomagnetic polarity epochs; Pribilof Islands, Alaska: Geological Society of America Bulletin, v. 77, p. 883-910.

Creager, J. S., Scholl, D. W., and others, 1973, Initial reports of the Deep Sea Drilling Project, v. 19: National Science Foundation; U.S. Government Printing Office, Washington, D. C., 913 p.

Davies, J. N., 1981, Seismic and volcanic risk [in the St. George basin and adjacent Aleutian Arc], section 3.5 in Hameedi, M. J., ed., Proceedings of a synthesis meeting; The St. George basin environment and possible consequences of planned offshore oil and gas development, Anchorage, Alaska, April 28-30, 1981: U.S. Department of Commerce, NOAA, Outer Continental Shelf Environmental Assessment Program (OCSEAP), and U.S. Department of Interior, Bureau of Land Management, p. 46-48.

Davies, J. N., and Jacob, K. H., 1981, A seismotectonic analysis of the seismic and volcanic hazards in the Pribilof Islands-Eastern Aleutian Islands region of the Bering Sea, in Environmental Assessment of the Alaskan continental shelf, annual reports of principal investigators for the year ending March 1981, v. 7, Hazards: U.S. Department of Commerce, NOAA, Outer Continental Shelf Environmental Assessment Program, (OCSEAP), and U.S. Department of Interior, Minerals Management Service, Research Unit 16, p. 1-124.

Demaison, G. J., 1981, Stratigraphic aspects of source bed occurrence, the organic facies concept, in AAPG geochemistry for geologists (Short Course Notes): American Association of Petroleum Geologists, 108 p.

Detterman, R. L., 1982, Late Mesozoic and Tertiary stratigraphy for the Alaska Peninsula [abs.]: Alaska Geological Society Symposium, Anchorage, Alaska, 1982, Proceedings, p. 5.

Espitalié, J., Madec, M., Tissot, B., Mennig, J. J., and Leplat, P., 1977, Source rock characterization method for petroleum exploration: Proceedings of the 9th Annual Offshore Technology Conference, Houston, Texas, v. 3, p. 439-448.

Flett, T. O., 1984, Organic geochemistry, in Turner, R. F., ed., Geological and operational summary, St. George Basin COST No. 2 well, Bering Sea, Alaska: U.S. Minerals Management Service OCS Report MMS 84-0018, p. 73-88.

Gardner, J. V., Dean, W. E., and Vallier, T. L., 1980, Sedimentology and geochemistry of surface sediments, Outer Continental Shelf, southern Bering Sea: Marine Geology, v. 35, no. 4, p. 299-329.

Gardner, J. V., Vallier, T. L., Dean, W. E., Kvenvolden, K. A., and Redden, G. D., 1979, Sedimentology and geochemistry of surface sediments and the distribution of faults and potentially unstable sediments, St. George Basin region of the Outer Continental Shelf, southern Bering Sea: U.S. Geological Survey Open-File Report 79-1562, 89 p.

Hammond, R. D., and Gaither, J. R., 1983, Anomalous seismic character, Bering Sea shelf: Geophysics, v. 48, p. 590-605.

Harbert, W. P., Feri, L. S., Cox, A., and Engebretson, D. C., 1985, Relative motions between Eurasia and North America in the Bering Sea region [abs.]: AAPG Bulletin, v. 69, no. 4, p. 665-666.

Harding, T. P., 1984, Graben hydrocarbon occurrences and structural style: AAPG Bulletin, v. 68, no. 3, p. 333-362.

Hillhouse, J. W., and Coe, R. S., in press, Paleomagnetic data from Alaska, in Plafker, G., and Jones, D. L., eds., Cordilleran Orogen, Alaska: Geological Society of America Decade of North American Geology, v. G-1.

Hood, D. W., and Calder, J. A., eds., 1981, The eastern Bering Sea shelf; Oceanography and resources: U.S. Department of Commerce, NOAA, Office of Marine Pollution Assessment, 2 v.

Hopkins, D. M., Scholl, D. W., Addicott, W. O., Pierce, R. L., Smith, P. B., Wolfe, J. O., Gershanovich, D., Kotenov, B., Lohman, K. E., Lipps, J. H., and Obradovich, J., 1969, Cretaceous, Tertiary, and early Pleistocene rocks from the continental margin in the Bering Sea: Geological Society of America Bulletin, v. 80, p. 1471-1480.

Hopkins, D. M., and Silberman, M. L., 1978, Potassium-argon ages of basement rocks from St. George Island, Alaska: U.S. Geological Survey Journal of Research, v. 6, p. 435-438.

House, L., and Boatwright, J., 1980, Investigation of two high stress-drop earthquakes in the Shumagin seismic gap, Alaska: Journal of Geophysical Research, v. 85, p. 7151-7165.

Howell, D. G., Crouch, J. K., Greene, H. G., McCulloch, D. S., and Vedder, J. G., 1980, Basin development along the late Mesozoic and Cainozoic California Margin, a plate tectonic margin of subduction, oblique subduction and transform tectonics, in Ballance, P. F., and Reading, H. G., eds., International Association of Sedimentologists, Special Publication no. 4, p. 43-62.

Hunt, J. M., 1979, Petroleum geochemistry and geology: San Francisco, W. H. Freeman and Company, 617 p.

Iijima, Azuma, 1980, Geology of natural zeolites and zeolitic rocks: Pure and Applied Chemistry, v. 52, p. 2115-2130.

Iijima, Azuma, and Utada, Minoru, 1983, Recent developments in the sedimentology of siliceous deposits in Japan, in Iijima, A., Hein, J. R., and Siever, R., eds., Siliceous deposits in the Pacific region: Amsterdam, Elsevier, Developments in Sedimentology no. 36, p. 247-282.

Jones, D. L., and Silberling, N. J., 1979, Mesozoic stratigraphy, the key to tectonic analysis of southern and central Alaska: U.S. Geological Survey Open-File Report 79-1200, 37 p.

Kvenvolden, K. A., Vogel, T. M., and Gardner, J. V., 1981, Geochemical prospecting for hydrocarbons in the Outer Continental Shelf, southern Bering Sea, Alaska: Journal of Geochemical Exploration, v. 14, p. 209-219.

Larson, J. A., 1984a, Paleontology and biostratigraphy, in Turner, R. F., ed., Geological and operational summary, St. George Basin COST No. 1 well, Bering Sea, Alaska: U.S. Minerals Management Service OCS MMS Report 84-0016, p. 24-40.

Larson, J. A., 1984b, Paleontology and biostratigraphy, in Turner, R. F., ed., Geological and operational summary, St. George Basin COST No. 2 well, Bering Sea, Alaska: U.S. Minerals Management Service OCS MMS Report 84-0018, p. 28-37.

Marlow, M. S., and Cooper, A. K., 1980, Mesozoic and Cenozoic structural trends under southern Bering Sea shelf: AAPG Bulletin, v. 64, p. 2139-2155.

Marlow, M. S., and Cooper, A. K., 1983, Wandering terranes in southern Alaska, the Aleutian microplate and implications for the Bering Sea: Journal of Geophysical Research, v. 88, no. B4, p. 3439-3446.

Marlow, M. S., Gardner, J. V., Vallier, T. L., McLean, H., Scott, E. W., and Lynch, M. B., 1979, Resource report for the proposed OCS Lease Sale No. 70, St. George Basin shelf area, Alaska: U.S. Geological Survey Open-File Report 79-1650, 79 p.

Marlow, M. S., Scholl, D. W., Cooper, A. K., and Buffington, W. C., 1976, Structure and evolution of the Bering Sea shelf south of St. Lawrence Island: AAPG Bulletin, v. 60, p. 161-183.

McIver, R. D., 1973, Hydrocarbons in canned muds from sites 185, 186, 189, and 191, Leg 19: in Initial reports of the Deep Sea Drilling Project, v. 19: National Foundation; U.S. Government Printing Office, Washington, D.C., p. 875-877.

McLean, H., 1979, Pribilof segment of the Bering Sea continental margin; A reinterpretation of Upper Cretaceous dredge samples: Geology, v. 7, p. 307-310.

Meyers, H., 1976, A historical summary of earthquake epicenters in and near Alaska: U. S. Department of Commerce, National Oceanic and Atmospheric Administration, Environmental Data Service, National Geophysical and Solar-Terrestrial Data Center, Boulder, CO. Cited in U.S. Minerals Management Service, 1982.

Miller, T., and Smith, R., 1977, Spectacular mobility of ash flows around Aniakchak and Fisher Calderas, Alaska: Geology, v. 5, p. 173-176.

Mohr, P., 1982, Musings on continental rifts, in continental and oceanic rifts: American Geophysical Union Geodynamics Series, v. 8, p. 293-309.

Packer, D. R., 1972, Paleomagnetism of the Mesozoic in Alaska: College, Alaska, University of Alaska, Ph.D. dissertation, 160 p.

Packer, D. R., and Stone, D. B., 1974, Paleomagnetism of Jurassic rocks from southern Alaska, and tectonic implications: Canadian Journal of Earth Science, v. 11, p. 976-997.

Page, R. A., Plafker, G., Fuis, G. S., Nokleberg, W. J., Ambos, E. L., Mooney, W. D., and Campbell, D. L., 1986, Accretion and subduction tectonics in the Chugach Mountains and Copper River Basin, Alaska, initial results of the trans-Alaska crustal transect: Geology, v. 14, p. 501-505.

Peters, K. E., 1986, Guidelines for evaluating petroleum source rock using programmed pyrolysis: AAPG Bulletin, v. 70, no. 3, p. 318-329.

Rea, D. K., and Duncan, R. A., 1984, Late Cretaceous and Eocene changes in the North Pacific spreading regime and possible consequences for Alaska [abs.]: 80th Annual Meeting of Cordilleran Section, Geological Society of America, May 30-June 1, 1984, Abstracts with Programs, v. 16, p. 329.

Reed, B. L., and Lanphere, M. A., 1973, Alaska-Aleutian range batholith, geochronology, chemistry, and relation to circum-Pacific plutonism: Geological Society of America Bulletin, v. 84, p. 2583-2610.

Rhodehamel, E. C., 1977, Sandstone porosities, in Scholle, P. A., ed., Geological studies on the COST No. B-2 well, U. S. Mid-Atlantic outer continental shelf area: U.S. Geological Survey Circular 750, p. 23-31.

Scholl, D. W., Buffington, E. C., and Hopkins, D. M., 1966, Exposure of basement rock on the continental slope of the Bering Sea: Science, v. 153, p. 992-994.

Scholl, D. W., Buffington, E. C., and Hopkins, D. M., 1968, Geologic history of the continental margin of North America in Bering Sea: Marine Geology, v. 6, p. 297-330.

Scholl, D. W., Buffington, E. C., and Marlow, M. S., 1975, Plate tectonics and the structural evolution of the Aleutian-Bering Sea region, in Forbes, R. B., ed., Contributions to the geology of the Bering Sea Basin and adjacent regions: Geological Society of America Special Paper 151, p. 1-31.

Scholl, D. W., and Hopkins, D. M., 1969, Newly discovered Cenozoic basins, Bering Sea shelf, Alaska: AAPG Bulletin, v. 53, p. 2067-2078.

Scholl, D. W., and Marlow, M. S., 1970, Diapir-like structures in the southeastern Bering Sea: AAPG Bulletin, v. 54, p. 1644-1650.

Smith, D. A., 1980, Sealing and nonsealing faults in Louisiana Gulf Coast salt basin: AAPG Bulletin, v. 64, no. 2, p. 145-172.

Stone, D. B., and Packer, D. R., 1977, Tectonic implications of Alaska Peninsula paleomagnetic data: Tectonophysics, v. 37, p. 183-210.

Stone, D. B., and Packer, D. R., 1979, Paleomagnetic data from the Alaska Peninsula: Geological Society of America Bulletin, v. 90, p. 545-560.

Stone, D. B., Panuska, B. C., and Packer, D. R., 1982, Paleolatitudes versus time for southern Alaska: Journal of Geophysical Research, v. 87, p. 3697-3707.

Sykes, L., 1971, Aftershock zones of great earthquakes, seismicity gaps, and earthquake prediction for Alaska and the Aleutians: Journal of Geophysical Research, v. 76, no. 32, p. 8021-8041.

Tissot, B., Durand, B., Espitalié, J., and Combaz, A., 1974, Influence of nature and diagenesis of organic matter in formation of petroleum: AAPG Bulletin, v. 58, p. 499-506.

Turner, R. F., McCarthy, C. M., Comer, C. D., Larson, J. A., Bolm, J. G., Banet, A. C., and Adams, A. J., 1984a, Geological and operational summary, St. George Basin COST No. 1 well, Bering Sea, Alaska: U.S. Minerals Management Service OCS Report MMS 84-0016, 105 p.

Turner, R. F., McCarthy, C. M., Comer, C. D., Larson, J. A., Bolm, J. G., Flett, T. O., and Adams, A. J., 1984b, Geological and operational summary, St. George Basin COST No. 2 well, Bering Sea, Alaska: U.S. Minerals Management Service OCS Report MMS 84-0018, 100 p.

Turner, R. F., McCarthy, C. M., Steffy, D. A., Lynch, M. B., Martin, G. C., Sherwood, K. W., Flett, T. O., Adams, A. J., 1984c, Geological and operational summary, Navarin Basin COST No. 1 well, Bering Sea, Alaska: U.S. Minerals Management Service OCS Report MMS 84-0031, 245 p.

U.S. Minerals Management Service, 1982, Final Environmental impact statement, proposed Outer Continental Shelf oil and gas lease sale, St. George Basin, 1 v.

Vallier, T. L., Underwood, M. B., Jones, D. L., and Gardner, J. V., 1980, Petrography and geologic significance of Upper Jurassic rocks dredged near Pribilof Island, southern Bering Sea continental shelf: AAPG Bulletin, v. 64, p. 945-950.

Weber, K. J., Mandl, G., Pilaar, W. F., Lehner, F., and Precious, R. G., 1978, The role of faults on hydrocarbon migration and trapping in Nigerian growth fault structures: Proceedings of the 10th Annual Offshore Technology Conference, Houston, Texas, v. 4, p. 2643-2652.

Whitney, J. W., and Wallace, W. K., 1984, Oceanic plate motions and the tectonic evolution of the Bering Sea shelf [abs.]: 80th Annual Meeting of Cordilleran Section, Geological Society of America, May 30-June 1, 1984, Abstracts with Programs, v. 16, p. 340.

Wilson, F. H., Detterman, R. L., and Case, J. E., 1985, The Alaska Peninsula terrane; a definition: U.S. Geological Survey Open-File Report 85-450, 17 p.

Woodward-Clyde Consultants, 1976, Report on preliminary geotechnical investigation, St. George Basin COST well, v. 1: Prepared for Atlantic Richfield Company, Dallas, Texas, 92 p.

☆ U.S. GOVERNMENT PRINTING OFFICE:1987-791-057/66000